AD-A130 093 RADIATION AND LASER POTENTIAL OF HOMO AND HETERONUCLEAR 1/1
RARE-GAS DIATOMIC..(U) CALIFORNIA UNIV SANTA BARBARA
QUANTUM INST W WALKER ET AL. DEC 82 AFOSR-TR-83-0559
UNCLASSIFIED F49620-77-C-0010 F/G 20/8 NL

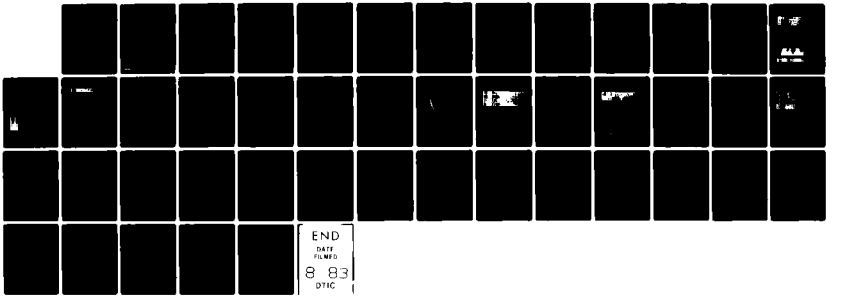

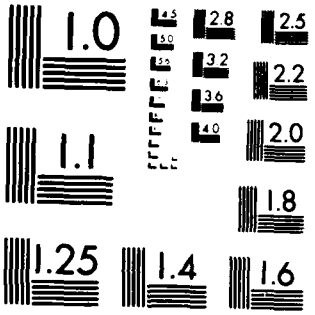

Unclassified
SECURITY CLASSIFICATION OF THIS PAGE (When Data Entered)

REPORT DOCUMENTATION PAGE		READ INSTRUCTIONS BEFORE COMPLETING FORM
1. REPORT NUMBER AFOSR-TR- 83-0559	2. GOVT ACCESSION NO.	3. RECIPIENT'S CATALOG NUMBER
4. TITLE (and Subtitle) Radiation and Laser Potential of Homo and Heteronuclear Rare-Gas Diatomic Molecules		5. TYPE OF REPORT & PERIOD COVERED Final Report 6. PERFORMING ORG. REPORT NUMBER
7. AUTHOR(s) William Walker Yoshio Tanaka		8. CONTRACT OR GRANT NUMBER(s) AFOSR 77-3137
9. PERFORMING ORGANIZATION NAME AND ADDRESS Quantum Institute University of California Santa Barbara, CA 93106		10. PROGRAM ELEMENT, PROJECT, TASK AREA & WORK UNIT NUMBERS 61102F 2303/B1
11. CONTROLLING OFFICE NAME AND ADDRESS AFOSR Building 410/NC Bolling AFB, Wash. D.C. 20332		12. REPORT DATE December 1982 13. NUMBER OF PAGES 44
14. MONITORING AGENCY NAME & ADDRESS(if different from Controlling Office)		15. SECURITY CLASS. (of this report) Unclassified 15a. DECLASSIFICATION/DOWNGRADING SCHEDULE

16. DISTRIBUTION STATEMENT (of this Report)

Distribution unlimited.

17. DISTRIBUTION STATEMENT (of the abstract entered in Block 20, if different from Report)

18. SUPPLEMENTARY NOTES

19. KEY WORDS (Continue on reverse side if necessary and identify by block number)

Vacuum Ultraviolet Spectroscopy
Rare-Gas Dimers
Excimers

20. ABSTRACT (Continue on reverse side if necessary and identify by block number)

High resolution emission spectra of the rare-gas dimers Ne_2^*, Ar_2^*, and Kr_2^* were studied in the vacuum ultraviolet region 500 - 1500 Å. Four band systems previously observed in all three dimers were studied in detail and classified in terms of the transition involved. Molecular constants and details of the dimer potential curves were determined.

DD FORM 1 JAN 73 1473

Unclassified
SECURITY CLASSIFICATION OF THIS PAGE (When Data Entered)

Final Scientific Report of
AFOSR Grant # 77-3137

Radiation and Laser Potential of Homo and Heteronuclear Rare-Gas Diatomic Molecules

W.C. Walker and Y. Tanaka
Quantum Institute
University of California
Santa Barbara, CA. 93106

December 1982

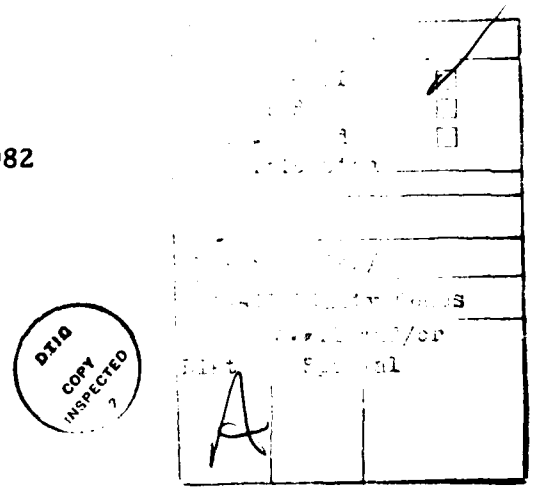

Research Objectives

The research consisted of a study of the emission spectra of the rare-gas dimers Ne_2, Ar_2 and Kr_2 in the vacuum ultraviolet between 500 and 2000 Å. The aim of the research was to observe new band systems, identify their origin and determine excited state energies and molecular parameters.

Summary of the Research:

The rare-gas dimers were studied in the order Ar_2, Ne_2 and finally Kr_2. The Ar_2 study began in 1976 and was completed in 1979. The results were published in references 1 and 2 attached. Ne_2 was studied from 1979 to 1981 and results were published in reference 3. Finally Kr_2 was studied until the termination of the grant. The results are still being analysed and a paper on Kr_2 will be published later.

A brief account of the main results for each dimer is given below.

A. Emission Spectrum of Argon Dimer

(1) Nine discrete band groups and eight diffuse bands are observed in the 1074 - 1127 Å region and identified as band system I, $^3\Sigma_u^+ \rightarrow X^1\Sigma_g^+$.[2] The transition is a bound-free type if the van der Waals minimum in the ground state potential curve is ignored. Each of the observed diffuse bands represents dissociation continua.

(2) Twenty-two bands, all diffuse, are observed in the 1067 - 1243 Å region. They form a single band progression which is identified as band system II, $^1\Sigma_u^+ \rightarrow X^1\Sigma_g^+$. Although all the bands appeared diffuse, the transition of this system is classified as bound-free type and each individual band represents a dissociation continuum.

(3) Seven bands, again all diffuse, are observed in a narrow region near the second resonance line of Ar I at 1048 Å. All bands are identified as belonging to band system III and each individual band represents a dissociation continuum. The transition involved in this system is $B5p\sigma(Ou^+) \rightarrow X^1\Sigma_g^+$ and the type of transition is classified as bound-free.

(4) Rotational analysis of the band system I has been made and rotational constants B_v and D_v were obtained in the upper state $^3\Sigma_u^+$. They are in the range $B_{v+1}=0.055-B_{v-6}=0.1051\ cm^{-1}$ and $D_{v+1}=1.0\times10^{-6}-D_{v-6}=0.30\times10^{-6}\ cm^{-1}$.

(5) Using these results an attempt has been made to depict the shape and position of the long range portion of the potential energy curves of the first two excited states $^3\Sigma_u^+$ and $^1\Sigma_u^+$ of Ar_2 relative to each other and to that of the ground state $X^1\Sigma_g^+$.

(6) The rotational analysis indicates that the coupling scheme in the lowest excited state is closer to the Hund-Milliken case b, than to case c, so that the symmetry of this state may be assigned approximately as $^3\Sigma_u^+$ rather than $^1{}_u$, O_u^-.

B. Emission Spectrum of Neon Dimer

(1) Band system I, $^1{}_u(^3P_2) \rightarrow X\ O_g^+(^1S_0)$, is observed in agreement with our previous results obtained in absorption. It is represented by a single band progression consisting of 10 bands covering the 745-781 Å range. Of the 10 bands, the three at shortest wavelengths are resolved into two sharp bands each and show rotational structure. The measured results of these resolved bands agree well with the absorption bands previously classified as band system I.

A simple calculation of the excitation energies of the upper vibration levels show the highest three observed levels $v'=v$, $v-1$, and $v-2$ are located above the separated atom limit by 142, 101 and 14 cm^{-1}, respectively. This indicates these three are quasibound resonating levels, that they predissociate to $Ne^*(3s^3P_2) + Ne(2p^6\ ^1S_0)$ and as a result, the spectrum would be expected to appear increasingly weaker toward higher vibrational level in emission while in absorption they should become increasingly stronger and diffuse toward the same direction. This behavior is in fact observed in both emission and absorption. The observation of quasibound resonating levels indicates the existence of a "hump" in the potential; in the present case the hump height is very close to $142 \pm 10\ cm^{-1}$, equivalent to the energy of the highest observed vibrational level measured from the separated atom limit of the same electronic state. Cohen and Schneider[4a] were the first to predict the existence of a potential hump in this state. Their calculated height is 0.108 eV (871 cm^{-1}), which is about six times the presently observed value.

(2) A long band progression consisting of 13 diffuse bands is observed in the 747 - 956 Å range and is designated as band system II. It belongs to the electronic transition $O_u^+(^3P_1) \rightarrow X\ O_g^+(^1S_0)$.[4a] This band system was missing in our absorption study.[2] A close inspection of the band progression revealed that one of the resonance lines at 743.7 Å is associated with a broad band in the immediate vicinity of its short wavelength side; this band shows a sudden intensity drop at about 741 Å. This and two other observations suggest existence of a potential hump in the upper state potential curve. Based on this suggestion, the calculated hump height is 670 50 cm^{-1} (0.083 eV) measured from the separated atom limit of the

upper state. Cohen and Schneider have predicted such a potential hump and their calculated value is 0.201 eV (1621 cm^{-1}).

(3) Four bands are observed immediately to the long wavelength side of resonance line at 735.8 Å and they form a short band progression. In the following three respects namely, general band appearance, strength, and location with respect to the resonance line, the band progression is analogous to that of band system III of the argon dimer. Thus, this band progression is similarly classified as system III in neon and assigned to the electronic transition $O_u^+(^1P_1) \rightarrow O_g^+(^1S_0)$. Although the band progression consists of only four bands, the $\Delta\nu$ vs n curve is reasonably smooth and converges near the resonance line, thus the energy difference between the n=4 band and the resonance line, which is $\Delta\nu = 544\ cm^{-1}$, is temporarily assumed as representing the dissociation energy of the upper state of the band system. The upper state potential curves of the $^1\pi(^3P)$ and $^1\Sigma(^1P)$ states and should have a small hump. The diffuse appearance of the observed bands might be attributed to the presence of the potential hump. Even though the band progression is limited to n=4, three of them, n=1, 2, 3, are strong, perhaps the strongest of all the three band systems. However, the intensity gradient in the progression is steep and because of this only four members are observed. The steep intensity gradient toward longer wavelength bands is qualitatively in agreement with the calculated results of Schneider and Cohen.[4b]

(4) When several torr of uncooled neon was excited with a weakly pulsed transformer discharge an additional band group was observed in the 779-792 Å range in association with a weak band system II. This new group consists of 9 bands each of which has its bandhead at the long wavelength

edge. Previously, we have reported similar band groups in Ar_2 and Xe_2. These three band groups are strikingly similar in several respects, for example, band appearance including direction of band heading, number of bands and their arrangement within the individual group, location of the individual group with respect to its own resonance line and experimental conditions such as excitation mode, gas pressure and temperature, under which the band group can be favorably excited. Because of these similarities, we suggest that these bands are produced in similar transitions in the individual dimers.

(5) When uncooled neon is excited in a Tesla coil discharge at pressures higher than ~ 15 torr, a weak emission continuum having a broad peak near 830 Å is observed in the 800 - 880 Å range. We believed it to be the second continuum of the neon dimer. A minor difference in the peak position compared to the previous value can be attributed to differences in the excitation mode between the two cases.

If the neon was cooled by liquid nitrogen but with the other conditions unchanged, an additional continuum is observed toward longer wavelengths. This continuum shows a broad peak around 905 Å, is slightly stronger than the other, and covers the range 870 - 970 Å. This continuum has not been previously observed and its origin is unknown at this stage.

(C) Emission Spectrum of Kr_2

Spectra were recorded in the range 1100 - 1500 Å in first order. Four band systems I ($1u \rightarrow X^1\Sigma_g^+$), II ($O_u^+ \rightarrow X^1\Sigma_g^+$), III ($O_u^+ \rightarrow X^1\Sigma_g^-$) and III* ($O_u^+ \rightarrow X^1\Sigma_g^+$).

Band system I begins at 1251 Å where it is most intense and extends to about 1332 Å.

Twenty two bands were observed.

Band system II extends from 1236 Å to 1251 Å where it becomes difficult to separate it from other overlapping lines. Eleven bands were recorded and catalogued.

Band system III was observed 1168 to 1170 Å and 13 members were identified and catalogued. The upper level for this band is formed from one ground state Kr atom and one atom excited with the configuration $4s^2 4p^5\ ^2P_{1/2}\ 5s$. This leads to a stable O_u^+ state having a shallow minimum. We found a dissociation energy $D_o = 442.8\ cm^{-1}$ for this state.

Three other band systems were observed for Kr_2, one between 1164 and 1161 Å, another near the short wavelength side of the first resonance line near 1235 Å and a diffuse progression near 1323 Å. The assignment of these bands is not yet clear.

Publications resulting from AFOSR 77-3137

1. Emission spectrum of Rare Gas Dimers in the Vacuum UV Region. I. Ar_2
   Y. Tanaka, W.C. Walker and K. Yoshino
   J. Chem. Phys. 70, 380 (1979).

2. Emission Spectrum of Rare Gas Dimers in the Vacuum UV Region. II. Rotational Analysis of Band System I of Ar_2
   D.E. Freeman, K. Yoshino, and Y. Tanaka
   J. Chem. Phys. 71, 1780 (1979).

3. Emission Spectrum of Rare Gas Dimers in the Vaccum UV Region. III. Ne_2
   Y. Tanaka and W.C. Walker
   J. Chem. Phys. 74(5), 2760 (1981).

4. Emission Spectrum of Kr_2 in the Vacuum Ultraviolet.
   Y. Tanaka and W.C. Walker (in preparation)

Personnel

W.C. Walker, Principal Investigator
Y. Tanaka, Co-Principal Investigator
Zeuglie Wu, Laboratory Assistant (1980-81)
Robert Zacher, Laboratory Assistant (1982)

Interactions

Emission Spectra of Rare Gas Dimers in the VUV
Paper presented at AFOSR/Molecular Dynamics Symposium, October 1979, by Y. Tanaka.

Emission Spectra of Kr_2 in the VUV Region
Paper to be presented at AFOSR/Molecular Dynamics Symposium, October, 1980, by Y. Tanaka.

Attendance at AFOSR Molecular Dynamics Symposium, November 9-11, 1981 (Y. Tanaka).

Emission spectrum of rare gas dimers in the vacuum UV regions. III. Ne_2

Y. Tanaka and W. C. Walker

Quantum Institute, University of California, Santa Barbara, California 93106
(Received 6 October 1980; accepted 13 November 1980)

Emission spectra of the neon dimer have been studied in the VUV region. Liquid nitrogen cooled neon was excited with a Tesla coil or transformer discharge. Three band systems I, II, and III were observed in the 735–1000 Å range and classified as produced by electronic transitions to the common ground state $X0_g^+(^1S_0)$ from the three low lying excited states $1_u(^3P_2)$, $0_u^+(^3P_1)$, and $0_u^+(^1P_1)$, respectively. Evidence for the existence of potential humps in the lowest two upper states were observed and the hump heights were calculated to be 142 ± 10 and 670 ± 50 cm^{-1}, respectively. Observations of additional spectra, a newly observed emission continuum and two diffuse band groups, are presented.

I. INTRODUCTION

In a previous study of the absorption spectrum of the argon dimer Ar_2 in the VUV region we observed three band progressions, two in the vicinity of the first resonance line at 1066.6 Å and one in the vicinity of the second resonance line at 1048.2 Å.[1] These progressions were designated as belonging to band systems I, II, and III in order of decreasing wavelength of the shortest wavelength band in each progression. The individual progressions originate in transitions from the common ground state: $X\,^1\Sigma_g^+(0_g^+)$ to the three low excited states: $4s\,^3\Sigma_u^+(1_u)$, $4s\,^1\Sigma_u^+(0_u^+)$, and $B\,5p\sigma(0_u^+)$,[2] respectively. We also studied the Ne_2 spectrum in absorption in the VUV region and found an unusual difference between it and the Ar_2 spectrum,[3] namely, while we predicted three band progressions in the Ne_2 spectrum such as those observed in Ar_2, band systems I and III were observed but system II was completely missing (see Figs. 2 and 3, Ref. 3). As will be described later (see Sec. III C), 10 out of the 12 diffuse emission bands reported in our previous study on the continuous emission spectrum of Ne_2[4] should correspond to band system II of Ar_2 but were not observed in absorption. One of the primary purposes of this work is to resolve this seemingly contradictory evidence by a careful study of the emission spectrum of the neon dimer in the same region.

Shortly after publication of our absorption work on the neon dimer, Cohen and Schneider[5(a)] reported a detailed theoretical calculation of the potential energy curves and molecular constants for the ground state and a number of the lowest excited states. They also reported calculations of the spectroscopic properties and radiative lifetimes of Ne_2.[5(b)] In this work we compare the spectroscopic results obtained in both emission and absorption with their calculations.

II. EXPERIMENTAL

The equipment and procedures used in this work are essentially the same as those described in our previous papers on the emission spectrum of the argon dimer in the VUV region.[6,7] In brief, the Ne_2 spectrum was photographed using two normal incidence type spectrographs, equipped with gratings of 2.0 and 6.65 m radius of curvature. The gratings were both ruled with 1200 lines/mm giving reciprocal dispersions in the first order of 4.2 and 1.2 Å/mm, respectively.

A π-shaped windowless discharge tube made of Pyrex, 8 mm in diameter and 30 cm in length, was mounted in front of the spectrograph slit. About 25 cm of the middle portion of the tube was cooled by liquid nitrogen in a Styrofoam container. Air Products and Chemical tank neon, purified by passing it through a liquid nitrogen cooled charcoal trap, was passed through the discharge tube and pumped out through the main vacuum system. The neon pressure in the tube was maintained in the range 1–40 Torr. The neon was excited by three different modes: (1) a transformer discharge using a transformer of 15 kV, 0.9 kV A; (2) an ac pulsed discharge using the same transformer combined with a 5 pF capacitor in parallel and an auxiliary spark gap in series[6]; and (3) a Tesla coil discharge using a CENCO leak tester.[6]

The neon dimer spectrum was photographed with Eastman-Kodak SWR and 101-01 plates and film. For the wavelength measurements CI, CII, OI, OII, and NI lines appearing as impurity spectra were used as references. The accuracy of the measurements for a sharp line is ± 0.01 and ± 0.002 Å for the low and high resolution spectrographs, respectively.

III. RESULTS AND DISCUSSION

A. General

The present work is restricted to the wavelength range 700–1000 Å, where three band systems I, II, and III of Ne_2 originating in transitions from the three low-lying excited states $1_u(^3P_2)$, $0_u^+(^3P_1)$, and $0_u^+(^1P_1)^0$ to the common ground state $X0_g^+(^1S_0)$, respectively, can be expected. The potential energy curves of these and other states, which are derived from the same separated atom limits as above, have been calculated by Cohen and Schneider,[5(a)] Berman and Kaldor,[10] and Iwata.[11] The results of one of Cohen and Schneider's calculations, which includes the effects of spin–orbit coupling, are shown in Fig. 1 [see also Figs. 1, 6, and 7, in Ref. 5(a)]. In the figure, the electronic transition for each of these three band systems is represented by a verti-

 0021-9606/81/052760-09$01.00

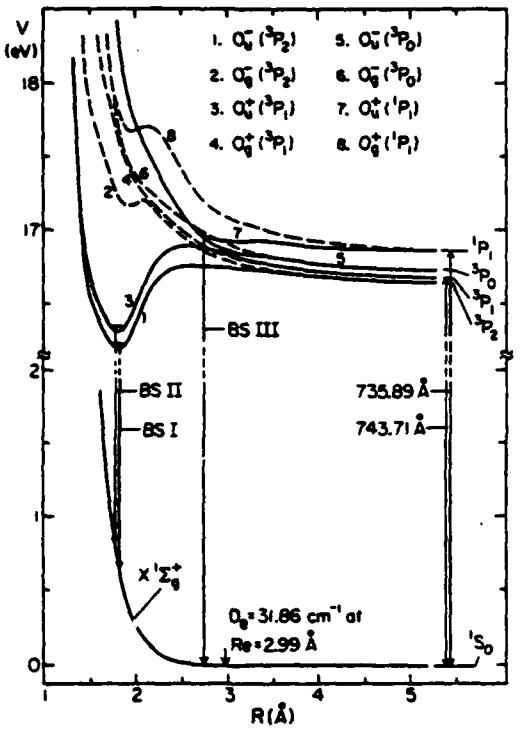

FIG. 1. Potential energy curves of Ne_2 for the low-lying excited states and the ground state. The curves were prepared by Cohen and Schneider at Los Alamos Scientific Laboratory [Ref. 5(a)]. This figure was prepared by combining their two figures: *Fig. 1 for the ground state and Fig. 8 for the excited* states with $\Omega = 0$ including spin–orbit coupling effects. The curve (1) should be replaced by curve (1), Fig. 7, Ref. 5(a), which represents $1_u(^3P_2)$, the upper state of the band system I. For the numerical values of D_e and R_e of the ground state see Table VII, Ref. 3.

cal line connecting the upper state and the ground state. This situation is very similar to that of the argon dimer.[6]

B. Band system I

Since there exists a close similarity between the potential energy curves of the argon[12,13] and neon[5(a),10,11] dimers, their spectra should be similarly located relative to their respective resonance lines. In Ne_2, three emission band progressions were observed in the region considered. One of them, which occupies the range 745–781 Å, consists of 10 bands, most of which appear diffuse. This band progression is classified as belonging to band system I and is assigned to the electronic transition $1_u(^3P_2) - X\,0_g^+(^1S_0)$. The band positions were measured at their estimated peaks using a low resolution spectrum and the results are listed in Table I. Part of the band progression is reproduced in the upper portion of Fig. 2. As is seen in the ure, the three bands with $n = 1$, 2, and 3 appear rathe rong and relatively narrow, while the others becom der and weaker as they approach longer wavelengt. his band progression was also photographed with high resolution spectrograph and a small portion of a magnified and reproduced in the top of Fig. 3. ure, each of the three bands $n = 1$, 2, and 3 are t resolved into four, two, and two discrete bands, respectively, most of them beginning to show rotational structures as seen in the top spectrum. Each resolved band has its head at its longest wavelength edge and degrades toward shorter wavelength. The resolved bands were measured at their heads and the results are listed in Table II. Also listed in the table are the results of the band groups which were observed in our absorption work (see Table I, Ref. 3). The agreement of the two results confirms that the two progressions of the band groups are identical.

TABLE I. Band system I with band groups measured at their estimated peaks.[a]

Group no. n	λ (Å)	I^b	ν (cm^{-1})	$\Delta\nu$	No. of bands[c]	Dissociation continuum[d]	Estimated total bandwidth (cm^{-1})[e]
1	745.1	6	134 210	130	2	Observed	120
2	745.8	10	134 080	260	4	Observed	180
3	747.3	5	133 820	380	2	Observed	230
4	749.4	4	133 440	440	0	Observed	290
5	751.9	2	133 000	550	0	Observed	330
6	755.0[f]	3	132 450	780	0	Observed	370
7	759.5[g]	2	131 670	920	0	Observed	440
8	764.8[h]	1	130 750	1220	0	Observed	
9	772.0[i]	1	129 530	1550	0	Observed	
10	781.4[j]	1	127 980		0	Observed	

[a] Bands photographed with the 2 m spectrograph in the second order and measured at estimated peaks.
[b] Estimated relative intensity within the system. Group no. 2, the strongest group, is assigned a relative intensity of 10.
[c] Number of discrete bands observed within the group.
[d] Dissociation continuum associated with the band group.
[e] Values are rough estimates; it depends on gas pressure, time of exposure, and excitation modes used.
[f] Obscured by $n = 3$ band of system II.
[g] Obscured by $n = 4$ band of system II.
[h] Superimposed upon $n = 2$, X_2 band system, and difficult to estimate the bandwidth.
[i] Superimposed upon $n = 4$, X_2 band system, and difficult to estimate the bandwidth.
[j] Difficult to estimate the bandwidth.

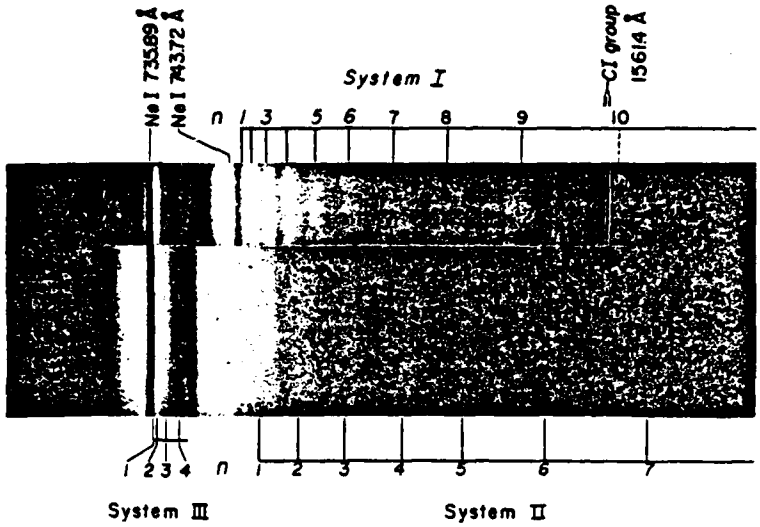

FIG. 2. Emission spectra of neon dimer, band systems I and II. The spectra were taken with the 2 m spectrograph equipped with a 1200 lines/mm grating in second order. The experimental conditions are as follows: for the top, p (Ne) = 15 Torr, cooled by liquid nitrogen, excited with Tesla coil, 3 min exposure time; and for the bottom, p (Ne) = 25 Torr, uncooled neon, excited with transformer discharge, 60 min exposure time. The slit widths were about 15 μ and Eastman 101-01 type film was used.

A simple calculation of the excitation energies of the upper vibrational levels shows that the highest observed three levels $v' = v$, $v-1$, and $v-2$ are located above the separated atom limit of the $1_u(^3P_2)$ state by 142, 101, and 14 cm^{-1}, respectively.[14] This indicates that these levels are all quasibound resonating levels[15(a)] and should all predissociate in some degree to $Ne^*(2p^5 3s\ ^3P_2) + Ne(2p^6\ ^1S_0)$ with increasing probability toward the high vibration level. As a result, the spectra will be expected to be observed either as abnormally weak in emission or abnormally strong and diffuse in absorption.[16] Figure 4 presents these bands observed in absorption. In the figure, one can clearly see evidence of predissociation effects, namely, two bands with $v' = v-2$ show rather sharp but weak heads with rotational structure beginning to be resolved, whereas the other two groups with $v' = v$ and $v-1$ are too strong and also too diffuse to show any rotational structure. In addition, the intensity difference between these three band groups becomes emphasized when the neon pressure is increased. The $v' = v-3$ band group is too weak to be reproduce ' in the figure. These observations confirm the existence of predissociation[16] and consequently the existence of a potential barrier in the upper state

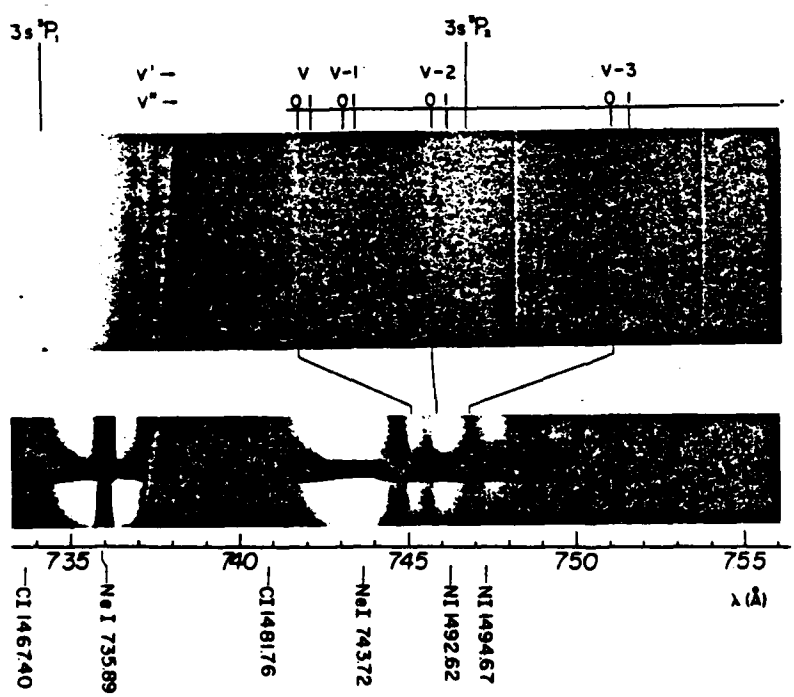

FIG. 3. Emission spectrum of neon dimer, band system I. The spectrum was taken with the 6.65 m spectrograph equipped with a 2400 lines/mm grating in second order. The experimental conditions are as follows: p (Ne) = 28 (top) and 10 (bottom) Torr, both liquid nitrogen cooled, excited with Tesla coil discharge, 15 μ slit width and 60 min exposure time. At least seven diffuse bands can be seen in the range 745–759 Å. The vibrational quantum numbers assigned are identical with those of the absorption spectrum (see Table II). For a weak and diffuse spectrum at about 744.2 Å see Sec. III G.

TABLE II. Band system I with resolved discrete bands measured at bandheads.[a]

Group no. n	v'	v''	λ (Å)	I^c	ν (cm^{-1})	λ (Å)[d]	I^d
1	v^b	0	745.12	7	134 207	745.113	10
		1	745.18	3	134 196	745.184	5
	$v-1$	0	745.34	4	134 167	745.341	3
		1	745.41	2	134 154	745.400	0
2	$v-2$	0	745.83	10	134 079	745.850	4
		1	745.90	3	134 066	745.920	1
3	$v-3$	0	746.82	1	133 901	746.830	0*
		1	746.89	0*	133 889	746.904	0*

[a]Discrete bands photographed with the 6.65 m spectrograph in the second order and measured at bandheads.
[b]The highest upper vibrational level observed in emission as well as in absorption.
[c]Estimated relative intensity within the band system in emission. The $(v-2, 0)$ band, which is the strongest, is assigned a value of 10.
[d]Reproduction of the absorption data[3] for comparison purposes.

$1_u(^3P_2)$. Since no upper vibrational level higher than $v' = v$ was observed at this stage (see Sec. III G) the energy at this level, which is 142 ± 10 cm^{-1} (0.018 eV) measured from the separated atom limit, should be very close to the height of the potential hump. Cohen and Schneider[5(a)] were the first to propose the existence of a potential barrier in this state and according to their calculation its height should be 0.108 eV (871 cm^{-1}) at $R_{max} = 2.58$ Å. The present value, based on the evidence of predissociation, is about one sixth of their value. A rotational analysis, which can not be done at this stage, will be required to obtain an accurate internuclear distance at the potential hump.

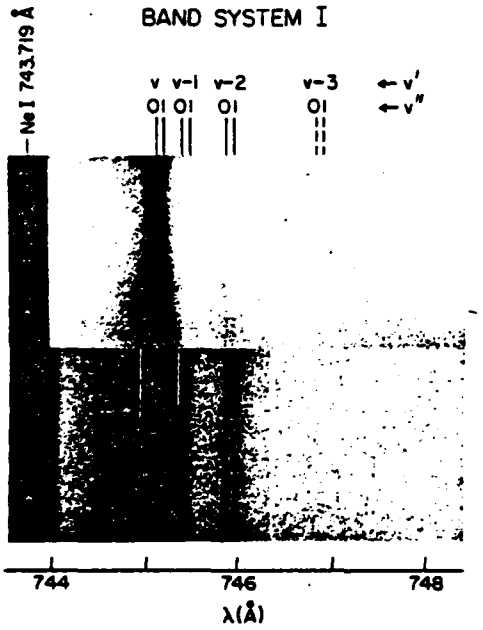

FIG. 4. Absorption spectrum of Ne_2, band system I showing the effect of predissociation. The spectrum was photographed with the 6.65 m spectrograph with a 1200 lines/mm grating in second order. The conditions are as follows: p(Ne) = 120 (top) and 194 (bottom) Torr, the neon was cooled at 77 °K, and a 15 μ slit width was used. Exposure times were 15 and 30 min for top and bottom, respectively. The neon continuum was used as the background source. Emission lines seen are Ne I lines at 1492.62, 1492.81, and 1494.67 Å, in first order.

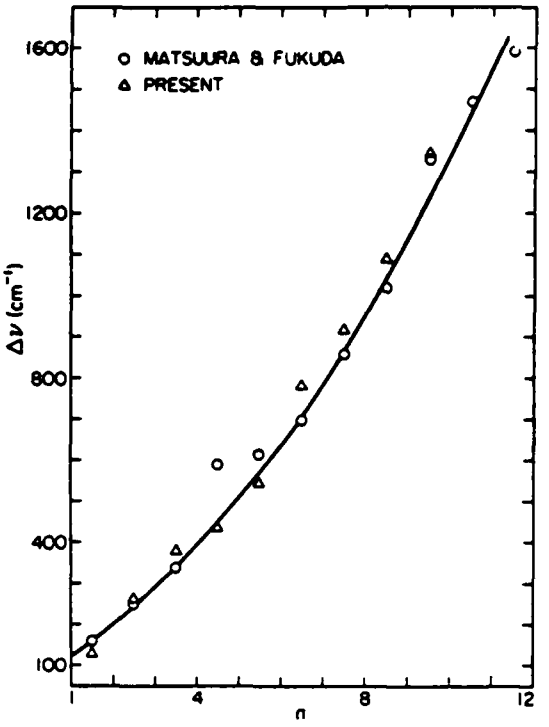

FIG. 5. $\Delta\nu$ vs n curve of band system I. The curve is drawn using the data by Matsuura and Fukuda.[17]

It was difficult for us to observe certain members of this band progression because of interference from the X_2 band system, which will be described later in Sec. III F. This interference was minimized by exciting liquid nitrogen cooled neon with a Tesla coil discharge at a pressure $p \leq 3$ Torr. Using a low current glow discharge of liquid nitrogen cooled neon at about 1 Torr, Matsuura and Fukuda[17] observed an undisturbed band progression which consisted of 12 bands in the range 745–798 Å. They classified this as belonging to the transition $1_u(^3P_2) - X\,0_g^+(^1S_0)$. The present results for band system I agree with theirs within their experimental error. The $\Delta\nu$ vs n curve for both sets of data is given in Fig. 5. Very recently, they also reported the existence of a potential hump in the upper state of band system I.[16] Based on the energy difference between the metastable neon atom $2p^5 3s(^3P_2)$ level and the observed shortest wavelength band at 745.0 Å, they estimated the height of the potential hump to be in the range $E = 0.02$–0.03 eV. Our value of 0.018 eV is close to their lower limit.

Matsuura and Fukuda[17] also reported a similar band progression in the argon dimer emission spectrum and our results on band system I of Ar_2[6] agree with theirs.

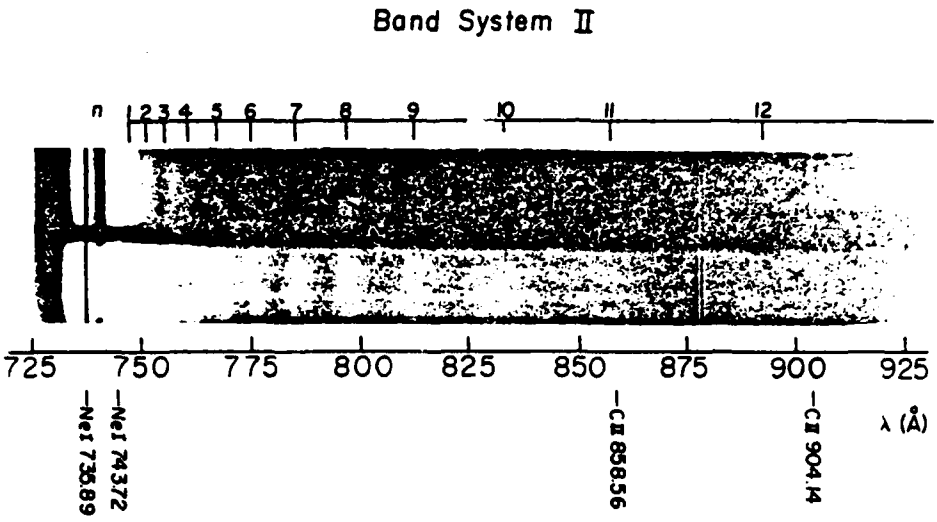

FIG. 6. Emission spectrum of Ne_2, band system II. The spectrum is taken with the 2 m spectrograph with 1200 lines/mm grating used in second order under the conditions; p(Ne) = 30 Torr, uncooled, excited with a transformer discharge, 20 μ slit width, and 30 and 120 min exposure times for the top and bottom spectra, respectively. Only a small portion of the $n = 13$ band is included in this figure.

Their results for the argon dimer spectrum provide additional support for our classification of band system I in the neon dimer in emission.

The electronic transition assigned to band system I in our earlier absorption study of Ne_2 (see Sec. III A. 1, Ref. 3) is incorrect and the upper state should be designated as $1_u(^3P_2)$ instead of $0_u^+(^3P_1)$ as shown in Fig. 1. This error originated primarily from the fact that band system II was not observed in the absorption spectrum (see Sec. III C).

C. Band system II

This band system belongs to the electronic transition $0_u^+(^3P_1) - X\,0_g^+(^1S_0)$. A typical spectrum of this system photographed with the low resolution spectrograph is reproduced in Fig. 6. It consists of a single progression of 13 broad bands and covers the range 746.7–956.5 Å, equivalent to 3.64 eV. Individual bands are quite diffuse without exception and their widths are broad and increase monotonically toward longer wavelengths. Their positions were measured at the estimated peaks and are listed in Table III. The $\Delta\nu$ vs n curve of the progression is shown in Fig. 7. Total bandwidths were estimated and included in Table III and plotted against n in Fig. 7. There are two intensity peaks in the progression, one at $n = 1$ and the other at $n = 10$ with a shallow minimum at $n = 6$ as seen in Fig. 6. It was reported previously[4] that the neon continuum in the VUV region has two intensity peaks, one at 744 Å and the other at 822 Å with a shallow valley at 775 Å. The two sets of estimates agree fairly well, indicating that the continuum and the present band progression both originate in the same electronic transition.

As seen in Fig. 2, the position of the $n = 1$ band of system II is located between the $n = 2$ and 3 bands of system I. In a transformer discharge of uncooled neon, system II will be excited together with system I but as the neon pressure is increased to p(Ne) ≥ 30 Torr the former becomes strong while the latter disappears except for its $n = 1$ band (see the top spectrum in Fig. 6). A close inspection of the spectrum photographed under the above condition suggests that the system II progression may not begin at the $n = 1$ band but rather it begins near 741 Å, where a steep intensity drop in the spectrum, which is seen in Figs. 2 and 6 was observed.

TABLE III. Band system II with bands measured at their estimated peaks.[a]

Band no. n	λ (Å)	I[b]	ν (cm^{-1})	$\Delta\nu$	Bandwidth (cm^{-1})[d]
1	746.7[e]	10	133 920	640	140
2	750.3	8	133 280	790	410
3	754.8	7	132 490	950	600
4	760.2	7	131 540	1060	720
5	766.4	5	130 480	1410	850
6	774.8	4	129 070	1710	980
7	785.2	5	127 360	1810	1330
8	796.5	6	125 550	2260	1580
9	811.1	6	123 290	2810	1900
10	830.0	7	120 480	3520	2250
11	855.0	5	116 960	4750	2720
12	891.2	4	112 210	7660	3820
13	956.5[f]	3	104 550		7500

[a] Bands photographed with the 2 m spectrograph in the second order.
[b] Estimated relative intensity within the band system. The strongest band at 746.7 Å is assigned a value of 10.
[c] The peak location is close to the average of $n = 2$ and 3 band groups of system I and the latter two used to appear superimposed upon the former.
[d] Roughly estimated total bandwidth.
[e] This band is partially out of range in Fig. 6.

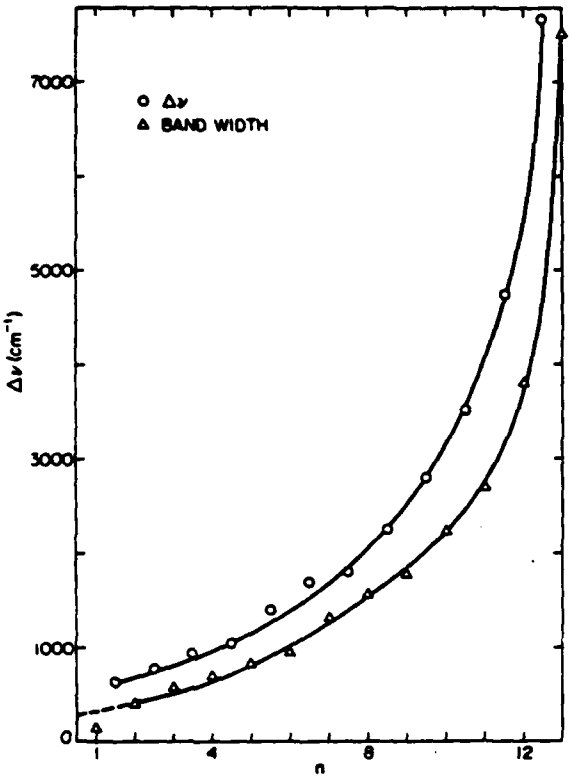

FIG. 7. $\Delta\nu$ vs n curve of the band system II. Estimated total bandwidth shown by Δ depends on several factors such as the mode of excitation, gas pressure, and exposure time.

This suggestion is supported by the following three points: (1) It was observed that the resonance line at 743.7 Å broadens toward short wavelengths with a flat-top type, but not an exponential type, intensity distribution down to about 741 Å, where it weakens rather sharply and disappears. The spectrum covered by the broadened resonance line will be called "broad emission band" hereafter. In most cases, the broad emission band was observed in association with system II and its strength increases in proportion to that of the band system II. No similar broad band was observed for the other resonance line at 735.9 Å; it simply decays exponentially toward short wavelengths though it is stronger and broader than the other. (2) The $\Delta\nu$ vs n curve shown in Fig. 7 suggests the existence of a few more bands immediately below the $n=1$ band. Three of these, at 743.7, (which will be superimposed upon the resonance line), 741.5, and 739.6 Å, were estimated by linear extrapolation of the $\Delta\nu$ vs n curve and it is found that they cover about the same range as that covered by the broad emission band. However, we were unable to distinguish them separately within the broad spectrum. The reason for this is probably due to the following factors: (a) the diffuse nature of these, like other members in the progression, combined with the narrow spacing between consecutive bands, (b) additional diffuseness originating from their quasibound resonating upper levels as will be described later, and (c) superposition of the broadened resonance line upon them. (3) *In the previous absorption work,*[3] an unexplained broad band was reported at about 741 Å (see Fig. 2, Ref. 3). This band is weak, with an appearance pressure of 10 Torr, and extends in both directions as the sample pressure increases. At a pressure of 80 Torr, for example, a narrow range of 738–744 Å becomes totally absorbed as shown in the same figure. This behavior is quite similar to that of the system I bands shown in Fig. 4, where the effect of predissociation becomes evident when the sample pressure is increased.

On the basis of the above discussion, it is suggested that the broad emission band may correspond to an emission spectrum produced in a transition to the ground state from upper vibrational levels above the separated atom limit of the $0_u^+(^3P_1)$ state. Here we have assumed that the characteristics of the two broad bands, one observed at 741 Å in absorption and the other, the broad emission band, both originate from the same cause, i.e., the predissociation at high vibrational levels of the $0_u^+(^3P_1)$ state. If the above suggestions are valid, the total number of vibrational levels of the upper state will be 16 and three of these at the highest energies should be quasibound resonating levels. Based on the above discussion, the upper state will have a potential hump with a height calculated to be 670 ± 50 cm^{-1} ($0.083 \pm 6\times10^{-3}$ eV) measured from the separated atom limit of the upper state. *The large error shown is caused* by the broad and diffuse nature of the spectra which results in uncertainty in the calculation. Cohen and Schneider's calculated hump height for this state is 0.201 eV (1620 cm^{-1}) at $R_{max} = 2.54$ Å.[5(a)] This value is about 2.3 times larger than ours. So far we have been unable to obtain any spectroscopic evidence which reconciles the difference between the two values.

In the previous absorption study[3] we were unable to observe band system II, whereas several bands belonging to band system I were observed though they were quite weak. It is known that the system II type of electronic transition, in general, produces a stronger spectrum than that of system I type [see Fig. 2, Ref. 5(b), for example]. This apparent inconsistency can be resolved in part by the suggestion made earlier, namely, the broad absorption band at 741 Å originates in transitions from the ground state to several high vibrational levels located above the separated atom limit of the upper state $0_u^+(^3P_1)$. Once the broad absorption band thus becomes a part of system II, the inconsistency mentioned above will disappear because this band is stronger than the $(v,0)$ band of system I which is the strongest in that system.[3] Incidentally, the upper vibrational levels of both the $(v,0)$ band of system I and the diffuse band in system II at 741 Å are also quasibound resonating levels[15(a)] on the basis of the above discussion. It should be mentioned here that the width of the upper state potential curve of system II is quite narrow compared with the corresponding curve in Ar_2 (shown in Fig. 1, Ref. 6) so that a small transition probability in absorption will persist to high upper vibrational levels, perhaps even up to those which lie beyond the separated atom limit. This would be an important factor in our inability to observe mutually separated

absorption bands even around the dissociation limit of the upper state.

Three more bands are observed toward longer wavelengths in this study than in the previous emission study[4]; all three are broad, particularly so for the $n=13$ band at 956.5 Å which covered an estimated range equivalent to about 0.91 eV. The shape of the individual bands is symmetric without exception. The best way to excite the band progression without disturbance by other band groups is to use a non-pulsed transformer discharge of uncooled neon at a pressure $p(\mathrm{Ne}) \geq 30$ Torr. It appears stronger if excited with a pulsed discharge but then strong disturbing band groups are simultaneously produced.

D. Band system III

Four bands were observed immediately to the long wavelength side of the second resonance line at 735.8 Å. Individual bands showed neither fine structure nor intensity degradation, so their positions were measured at their estimated peaks; the results are listed in Table IV. In general appearance, strength, and location with respect to the resonance line, these bands are analogous to those of band system III of the emission spectrum of the argon dimer.[6] Thus, this band progression is also designated as band system III of the neon dimer. It is thus assigned to the transition from the excited state $0_u^+(^1P_1)$ to the ground state. A spectrum of this system is seen in Fig. 2 together with the other two systems I and II. The $\Delta\nu$ vs n curve is shown in Fig. 8. If the $n=4$ band, the weakest and the longest wavelength band in the progression, is assumed to originate in the $v'=0$ level, then the sum of $\Delta\nu$'s in the table, i.e., 544 cm^{-1} (0.0674 eV), gives a value close to the dissociation energy D_0 of the upper state [see curve 7, Fig. 6, Ref. 5(a)]. As included in Table IV, only two members of the same v' band progression were observed in absorption, while in this work two more members are added toward longer wavelengths. Thus, the presently estimated value $D_0 = 544$ cm^{-1} should be closer to the real value than the one estimated in the absorption work [see Ref. 17 cited in Ref. 5(a)].

TABLE IV. Band system III with bands measured at their estimated peaks.[a]

Band no. n	λ (Å)	I[b]	ν (cm^{-1})	$\Delta\nu$	λ (Å)[d]	v'/v''
	735.89[c]		135 889	75		
1	736.30	10	135 814	92	736.182	$v/0$
					736.257	$v/1$
2	736.80	8	135 722	147	736.498	$v-1/0$
					736.573	$v-1/1$
3	737.60	4	135 575	230		
4	738.85	1	135 345			

[a] Bands photographed with the 2 m spectrograph in the second order.
[b] Estimated relative intensity within the system. The $n=1$ band, the strongest, is assigned a value of 10.
[c] Second resonance line of Ne, adopted from R. L. Kelly and L. J. Palumbo, NRL Report 7599, NRL, Washington, D.C. (1973).
[d] Reproduction of the previous absorption data[3] for comparison purposes.

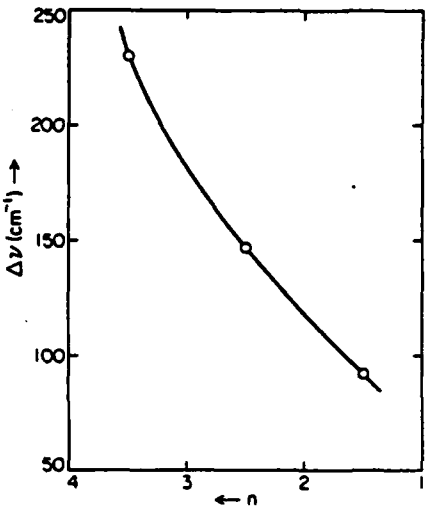

FIG. 8. $\Delta\nu$ vs n curve of the band system III.

As indicated by Cohen and Schneider,[5(a)] the upper state potential curve of this system is formed by two curves: One belongs to $^3\Pi_u(^3P)$ and the other to the $^1\Sigma_u^+(^1P)$ state, crossed at $R=2.75$ Å [see Figs. 3 and 6, Ref. 5(a)]. The resulting curve shows a shallow potential well with its minimum at $R_e=2.70$ Å. Though the presently observed band progression is limited in number and range, the intensity of the three shortest wavelength bands is strong, perhaps stronger than either of the other two systems I and II.

As indicated in Table IV, the intensities of the individual bands become rapidly weakened toward longer wavelengths. Qualitatively, this evidence is in agreement with the variation of the dipole transition matrix element with internuclear separation in this band system as calculated by Schneider and Cohen [see Fig. 2, Ref. 5(b)]. So far, no discrete bands have been observed in the region immediately to the short wavelength side of the resonance line either in emission or in absorption.[3] The evidence above, however, does not necessarily indicate the absence of dimer spectra there because even if they were the spectra would be seriously obscured by the strong and broadened resonance line.

E. Band system X_1

When several Torr of uncooled neon was excited with a weakly pulsed transformer discharge, another band group was observed in the 779–792 Å range together with band system II. This band group consists of nine bands, each of which appears slightly diffuse, but with clear degradation toward short wavelengths. We have designated this group as band system X_1. The positions measured at their heads are listed in Table V.

It is difficult to offer a conclusive explanation for the origin of this band system. Nevertheless, we suggest

TABLE V. Band systems X_1 and X_2 with bands measured at their peaks.[a]

Band no. n	λ (Å)	I^b	ν (cm^{-1})	Remarks
			X_1 band system	
1	778.8	10	128 400	Broad, shades toward blue
2	779.9	10	128 220	Broad, shades toward blue
3	783.3	8	127 660	Broad, shades toward blue
4	783.9	8	127 560	Broad, shades toward blue
5	786.5	6	127 140	Broad, shades toward blue
6	787.9	6	126 910	Broad, shades toward blue
7	789.2	4	126 710	Broad, shades toward blue
8	790.8	3	126 450	Narrow, no shading
9	792.3	1	126 210	Broad, shades toward red
			X_2 band system	
1	764.2	6	130 850	Broad, shades toward blue
2	765.4	7	130 650	Broad, shades toward blue
3	771.2	10	129 660	Broad, shades toward blue
4	772.2	10	129 500	Broad, shades toward blue
5	772.9	2	129 380	Narrow, shades toward blue
6	773.5	4	129 280	Narrow, no shading
7	774.1	2	129 182	Narrow, no shading
8	774.8	2	129 060	Narrow, no shading
9	775.3	6	128 980	Narrow, no shading
10	775.8	2	128 890	Narrow, no shading
11	776.4	5	128 790	Narrow, no shading
12	777.3	4	128 650	Narrow, no shading
13	778.5	2	128 480	Narrow, no shading
14	779.3	4	128 320	Narrow, no shading

[a]Bands photographed with the 2 m spectrograph in the second order.

[b]Estimated relative intensities within each system $n = 1, 2$ in the X_1 and $n = 3, 4$ in the X_2 system are given reference values of 10, the strongest.

that the band group originates in a transition comparable to that of band system X of Ar_2[6] and of the Xe_2 band group reported by us in the 1584–1621 Å range.[19] The above suggestion is based on the close similarities observed in the three band groups with respect to (1) their spectral appearance, (2) the band arrangement within each group, and (3) the experimental conditions under which the spectrum can be strongly excited.

F. Continuous spectra and band system X_2

When uncooled neon was excited with a Tesla coil discharge at pressures p(Ne) ≥ 15 Torr, a continuous emission spectrum was observed in the 800–880 Å range with a broad peak at about 830 Å. This continuum is always associated with the weak band system II. The peak position of the continuum is practically coincident with the $n = 10$ band of system II but is not in agreement with the second continuum peak reported at 822 Å.[4] Despite the discrepancy, we think the present continuum belongs to band system II and that the discrepancy could be attributed to the difference in the excitation modes used.

If the neon was cooled by liquid nitrogen keeping other conditions unchanged, an additional continuum, which is stronger and wider than the other, was observed toward longer wavelengths. This continuum has its peak at about 905 Å and covers the 870–970 Å range. It was also observed in the same spectrum that the system II bands lost intensity considerably but the system I band gained in intensity. The origin of the continuum is as yet unknown. Since whenever the continuum is strongly excited, the early members ($n = 1$ to 4) of band system I are also strongly excited, it seems quite probable that the continuum is produced by transitions from the same upper vibrational levels as are those that produce the early members of band system I to the ground state. It should be noted that with this interpretation the continuum transitions take place from the repulsive branch of the upper potential curve to the ground state where the slope of the potential curve is quite steep (see Fig. 1).

It seems practically certain that this continuum will not originate in transitions from the bottom part ($v = 0$) of the upper state potential well to the ground state because, if so, the energy difference $\Delta E = 1.2$ eV, of the two observed continua with peaks at 830 and 905 Å, respectively, is too large in comparison with the electronic energy difference $\Delta E = 0.12$ eV between the two excited states $0_u^-(^3P_1)$ and $1_u(^3P_2)$, as calculated by Cohen and Schneider.[5(a)] Using high speed protons, Steward *et al.*[20] excited neon and observed a new continuum with its peak at 1000 Å. This observation was confirmed shortly thereafter by Leichner *et al.*[21,22] using high speed electron excitation. Both groups suggest that this continuum originates from a different transition than does the 850 Å continuum, the VUV neon continuum.[4] Schneider and Cohen[5(b)] suggest that the 1000 Å continuum could belong to the transition identical to band system I because "the lifetime of the upper state decreases significantly as the vibrational energy increases, and the wave function has more amplitude at the intermediate distances where the transition moment is larger."

We observed that the two continua with peaks at 905 and 822 Å appear always in association with a strong band group which consists of 14 bands and covers the narrow range 764–779 Å. Since the appearance of the group is similar to that of band system X_1, not only in its individual bands but also as a whole group, it is designated temporarily as band system X_2. The positions of the band peaks measured are included in Table V. As in the case of X_1, we are unable to offer a reliable explanation for the origin of this new band group at this time. It is possible that these new band systems may be produced by an impurity. However, this seems unlikely, since under experimental conditions where the continua and the two band systems appeared strong, impurity atomic lines such as O I, N I, C I, or C II became significantly weaker.

G. Additional spectra

In Fig. 3, one may notice an unclassified narrow and weak emission spectrum at about 744.2 Å in the bottom two spectra. At a glance, it appears to correspond to the $v' = v + 1$ band group in band system I if one ignores the $v - 1$ group temporarily. In an attempt to learn its origin, it was studied further using the 2 m spectrograph. The results are as follows: (1) The spectrum can be observed only when liquid nitrogen cooled neon is excited at a pressure in a range 1–3 Torr. (2) there is no pref-

erence for excitation mode, (3) the spectrum is observed together with a few members $n = 1$, 2, and 3 of band system I, and (4) the spectrum disappears when the neon pressure exceeds about 3 Torr, although the system I bands become stronger as the neon pressure increases. Two tentative explanations of this spectrum are as follows: (1) It could represent a member of a set of Rowland ghosts of the strong resonance line at 743.7 Å. (2) It is possible, however that the spectrum could represent one of the higher members, probably a band group with $v' = v + 1$, of band system I. If the latter is the case, the potential hump height of the upper state of system I will be 310 ± 10 cm^{-1} [$(0.038 \pm 12 \times 10^{-4}$ eV]. A more detailed study of the spectrum with a high resolution instrument is thus highly desired.

ACKNOWLEDGMENTS

This work was supported by the Air Force Office of Scientific Research under contract AFOSR 77-3137. Part of this work was carried out at Air Force Geophysics Laboratory and one of the authors (Y.T.) is grateful to members of the laboratory for their help.

The authors are thankful to Dr. James S. Cohen and Dr. Barry Schneider for permission to use their potential curves of neon dimer. We are also thankful to Dr. K. Yoshino and Dr. D. E. Freeman for their help in taking the high resolution neon dimer emission spectrum for us. We are also grateful to Mr. Thomas Hofmann in our institute for his great interest and critical discussions throughout the course of the research.

[1] Y. Tanaka and K. Yoshino, J. Chem. Phys. 53, 2012 (1970).
[2] For electronic state designation see R. S. Mulliken, J. Chem. Phys. 52, 5170 (1970).
[3] Y. Tanaka and K. Yoshino, J. Chem. Phys. 57, 2964 (1972).
[4] Y. Tanaka, A. S. Jursa, and F. J. LeBlanc, J. Opt. Soc. Am. 48, 304 (1958).
[5] (a) James S. Cohen and Barry Schneider, J. Chem. Phys. 61, 3230 (1974); (b) Barry Schneider and James S. Cohen, *ibid.* 61, 3240 (1974).
[6] Y. Tanaka, W. C. Walker, and K. Yoshino, J. Chem. Phys. 70, 380 (1979).
[7] D. E. Freeman, K. Yoshino, and Y. Tanaka, J. Chem. Phys. 71, 1780 (1979).
[8] R. E. Huffman, Y. Tanaka, and J. C. Larrabee, Appl. Opt. 2, 617 (1963).
[9] Electronic state designation used by Cohen and Schneider in Ref. 5(a) is adopted in this work. See also Ref. 2.
[10] Michael Berman and Uzi Kaldor, Chem. Phys. 43, 375 (1979).
[11] Sueshiro Iwata, Chem. Phys. 37, 251 (1979).
[12] D. C. Lorents, Physica (Utrecht) C 82, 19 (1976); see also references therein.
[13] Roberta P. Saxon and Bowen Liu, J. Chem. Phys. 64, 3291 (1976).
[14] The calculation was made using the previously assigned vibrational quantum numbers and molecular constants included in Table VII, Ref. 3.
[15] (a) K. M. Sando and A. Dalgarno, Mol. Phys. 20, 103 (1971); (b) K. M. Sando, *ibid.* 21, 439 (1971); (c) K. M. Sando, *ibid.* 23, 413 (1972).
[16] G. Herzberg, *Spectra of Diatomic Molecules* (Van Nostrand, New York, 1950), pp. 405–430.
[17] Yoshio Matsuura and Kuniya Fukuda, J. Phys. Soc. Jpn. 46, 1397 (1979).
[18] Yoshio Matsuura and Kuniya Fukuda (private communication).
[19] Y. Tanaka, J. Opt. Soc. Am. 45, 710 (1955).
[20] T. E. Stewart, G. S. Hurst, T. E. Bortner, J. E. Parks, F. W. Martin, and H. L. Weidner, J. Opt. Soc. Am. 60, 1290 (1970).
[21] P. K. Leichner, Phys. Rev. A 8, 815 (1973).
[22] P. K. Leichner, J. D. Cook, and S. J. Luerman, Phys. Rev. A 12, 2501 (1975).

Emission spectrum of rare gas dimers in the vacuum uv region. I. Ar_2

Y. Tanaka and W. C. Walker

Quantum Institute, University of California, Santa Barbara, California 93106

K. Yoshino

Harvard–Smithsonian Center for Astrophysics, Cambridge, Massachusetts 02138
(Received 24 August 1978)

Emission spectra of the argon dimer have been studied in the vuv region. Liquid nitrogen cooled argon was excited with a rf (Tesla coil) discharge. Four band systems, *I*, *II*, *III*, and *x*, were observed in the 1000–1500 Å region and classified as transitions to the common ground state $X\,^1\Sigma_g^+$ (O_g^+) from the upper states $A4s\,^3\Sigma_u^+(1_u)$, $A4s\,^1\Sigma_u^+(O_u^+)$, $B5p\sigma(O_u^+)$ and *x*, respectively. Except for band system *I*, they consisted entirely of diffuse bands.

I. INTRODUCTION

The emission spectrum of rare gas dimers in the vuv region has been studied in the past primarily with the aim of developing continuous light sources in that region.[1–7]

In recent years rare gas dimers have been investigated by molecular beam scattering,[8–11] by absorption spectroscopy in the vuv region,[12–15] by theoretical calculations,[16–24] and other means.[25] Excellent results with good mutual agreement have been obtained but with some exceptions the studies were restricted to the ground and a few low lying excited electronic states.

The current demand for production of high energy, short wavelength lasers has stimulated interest in rare gas elements and their dimers which seem destined to play an important role in this field in the future. For these reasons, a renewed study of rare gas dimer spectra in emission in the vuv region was undertaken, to provide information about the excited states of dimers and dimer ions.

II. EXPERIMENTAL

Argon was excited by a Tesla coil discharge with a CENCO leak tester, No. 80721, 50 kV, 4–5 MHz or No. 80730, 50 kV, 0.5 MHz. A windowless Pyrex discharge tube, 15 mm in diameter and 30 cm in length, was mounted in front of the spectrograph slit and about 20 cm of its middle portion was cooled by liquid nitrogen in a Styrofoam container. Aluminum foil, ~2 cm wide, wrapped around the tube at its far end served as an electrode for the discharge. Two additional Al electrodes were attached to the discharge tube to allow for conventional transformer discharges. Spectra from the latter were used for comparison purposes.

AIRCO high purity tank argon was introduced into the discharge tube without further purification. It was pumped through the slit by a differential pumping system[26] preceding the main system of the spectrograph. The argon pressure in the discharge tube was maintained in a range 0.1 ~ 70 torr. We find that with a Tesla coil discharge the argon dimer spectrum becomes discernible at about 0.1 torr of argon. It increases intensity as the pressure increases and reaches a maximum at about 15 torr, then it decreases with further pressure increase becoming indiscernible at about 70 torr. It is interesting to compare this result with those obtained from other modes of excitation.[2–7]

Two vuv spectrographs, one equipped with a 2 m and the other with 6.65 m radius of curvature grating both ruled with 1200 lines/mm, were used most often. The reciprocal dispersion was 4.2 and 1.2 Å/mm in first order, respectively. Information on other grating used is noted in the figure captions. Eastman Kodak SWR and 105-05 plates and film were used. Cu II lines produced by a hollow cathode lamp were used as standards for the spectrum taken with the 6.65 m spectrograph in the second order while C I and N I impurity lines produced by the Tesla coil discharge of argon were used for the 2 m spectrograph. The estimated accuracy of the wavelength measurements is ±0.002 and ±0.01 Å for a sharp line, respectively.

III. RESULTS

A. General

In addition to the second continuum reported previously,[4] four emission band systems were observed in this work in the 1050–1500 Å region. These are band systems I (1073–1128 Å), II (1067–1243 Å), III (1050–1057 Å), and *x* (1111–1157 Å). The first three are produced by transitions to the common ground state $X\,^1\Sigma_g^+(O_g^+)$ from the excited states, $A4s\,^3\Sigma_u^+(1_u)$, $A4s\,^1\Sigma_u^+(O_u^+)$, and $B5p\sigma(O_u^+)$, respectively. The orgin of the band system *x* is unknown at this time (see Sec. III E). The method of classification of the band systems adopted here is identical to that in absorption work.[12(b)] Band system I consists of discrete and diffuse bands but systems II, III and *x* consist entirely of diffuse (structureless) bands.

Figure 1 shows potential energy curves of the argon dimer prepared by Lorents and Olson[27] for the electronic states which are derived from the separated atom limits: Ar, $3s^23p^6\,^1S_0 + Ar^*$, $3p^5(^2P^0_{3/2})\,4s$, $J = 2, 1$; Ar, $3s^23p^6\,^1S_0 + Ar^*$, $3p^5(^2P^0_{1/2})\,4s'$ $J = 0, 1$; and $(Ar, 3s^23p^6\,^1S_0)^2$, the ground state.[28]

 0021-9606/79/010390-12$01.00

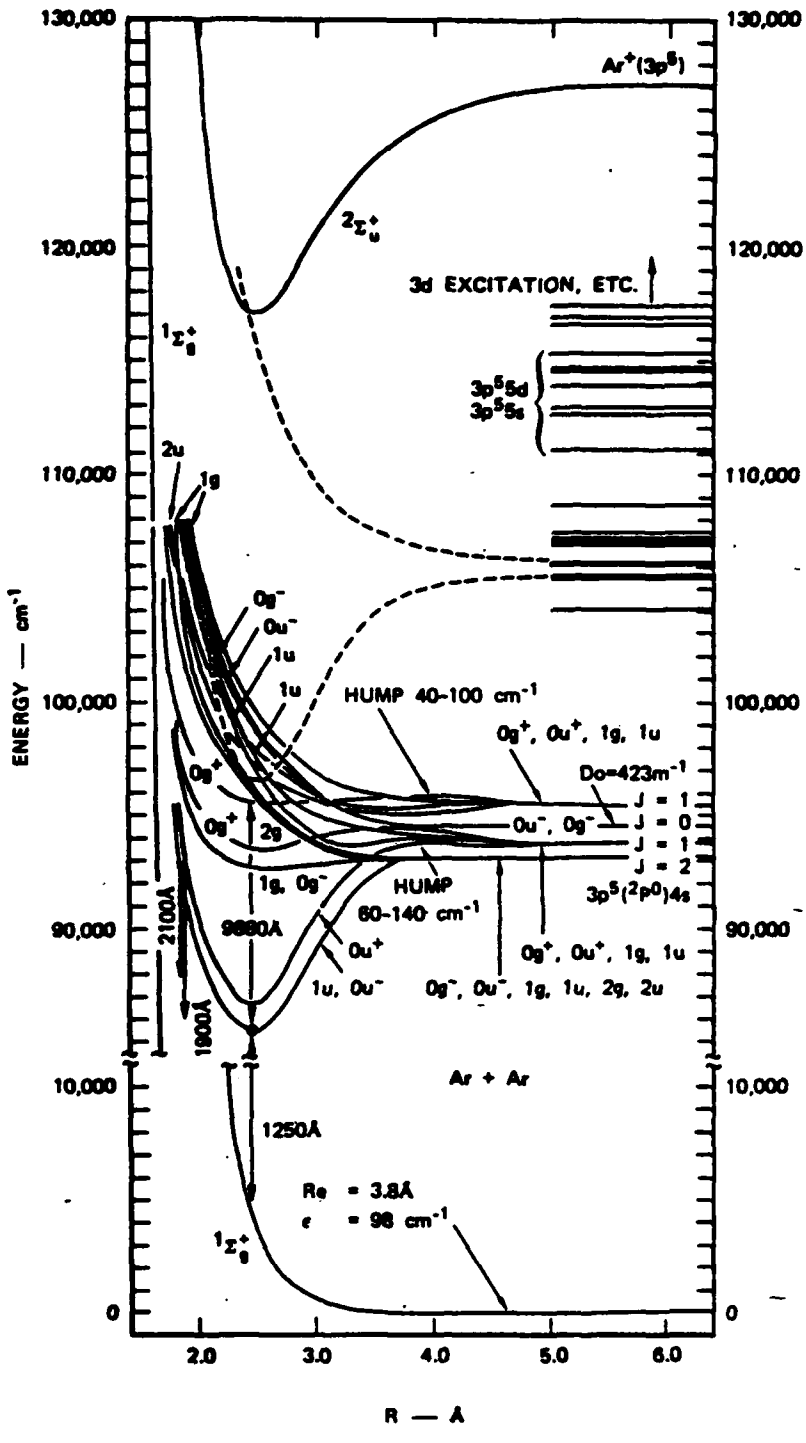

FIG. 1. Potential energy curves of Ar_2 for the low lying excited states. The curves were prepared by Lorents and Olson at Stanford Research Institute, Ref. 27. The two lowest excited states should be $4s\,^3\Sigma_g^+(1_g)$ and $4s\,^2\Sigma_g^+(0_g^+)$. Among the four curves derived from atom combination, $4s\,'J=1+3p^6J=0$, the lowest will be $B5p\sigma(0_g^+)$ (see Ref. 19). The arrow from $D_0=423\ cm^{-1}$ should be pointed to $J=1$ level [see Ref. 12(b)].

B. Band system I

Since band systems I and II occupy nearly the same wavelength region their overlapped spectrum makes classification difficult. This problem, however, was eliminated by using a mixture of argon with excess helium instead of pure argon. In the spectrum thus obtained, band system II becomes either considerably weakened or completely disappears leaving system I isolated. The preferred pressure ratio of the mixture is $p(Ar):p(He) \simeq 1:20$ torr, although it is not critical. One can also use neon instead of helium, though the former is less efficient than the latter. Figure 2 shows spectra of the two band systems I and II photographed under four different conditions with argon alone (top two) and argon and helium mixture (bottom two). Densitometer traces

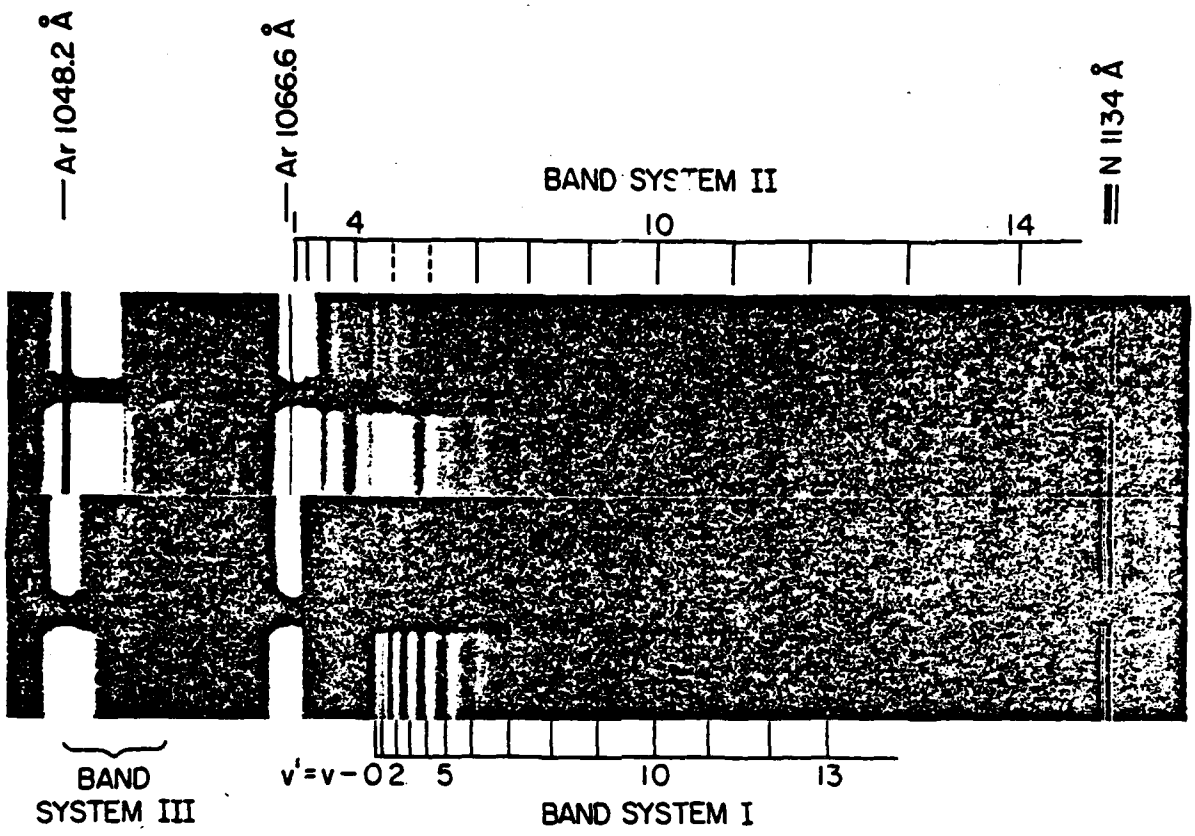

FIG. 2. Emission spectra of argon dimer, band systems I and II. Spectra were taken with a 2 m spectrograph, in second order, equipped with a 1200 line/mm grating. The experimental conditions are from top to bottom: (a) $p(Ar) = 3$ torr, exposure time = 2 min; (2) $p(Ar) = 15$ torr, exposure time = 10 min; (3) $p(Ar) = 1$ torr + $p(He) = 20$ torr, exposure time = 3 min; (4) $p(Ar) = 1$ torr + $p(He) = 20$ torr, exposure time = 20 min. All spectra are taken using liquid nitrogen cooled sample gas excited with Tesla coil discharge. The slit width was 15μ and Kodak film of 105-05 type emulsion was used.

of similar spectra are presented in Fig. 3. We were not successful in finding suitable conditions to isolate system II from the mixed spectrum. It should be mentioned that when band system I is isolated, the second continuum (see Sec. IV) becomes extremely weak at the same time. This indicates that the contribution of the band system I transition to the production of the second continuum is very small, if any.

A previous absorption spectrum study of the argon dimer[12(b)] suggested the existence of a relatively weak emission band system, system I, which is produced by the transition $A4s\,^3\Sigma_u^+(1_u) - X\,^1\Sigma_g^+(0_g^+)$ and begins at about 1073 Å extending toward long wavelengths. In this work seventeen band groups are observed in this system in the region 1073–1128 Å. The spectrum is reproduced at the bottom in Fig. 2 and a densitometer trace is shown at the top in Fig. 3. From a spectrum photographed with the 2 m spectrograph, the estimated peaks of the band groups were measured and results are given in Table I. Each individual band group belongs to one of the three categories as follows: (1) consists of one or more discrete bands alone; (2) consists of several discrete bands and a diffuse band; and (3) consists of a diffuse band alone. As indicated in Table I, band groups 1–6 belong to category (1), band groups 7–9 to category (2) and band groups 10–17 to category (3). The emission spectrum of the discrete bands taken with the 6.65 m spectrograph is reproduced in Fig. 4 at the top. The spectrum at the bottom in this figure shows the same bands in absorption taken with the same spectrograph. In the figure, the individual bands consist of reasonably well resolved rotational structures with band heads at the long wavelength edge degrading toward the opposite direction without exception. The wavelengths measured at the band heads are listed in Table II. In the table, previous results[12(b)] obtained from the absorption spectrum of system I are also listed for comparison. The agreement between the two is excellent.

In Fig. 4 one can also see the one to one correspondence between the rotational lines of the same band photographed in emission and in absorption. Accordingly, there is no question that the presently observed emission bands are identical with those of system I observed and so classified in absorption and one can safely conclude that the emission bands are produced by the transition $A4s\,^3\Sigma_u^+(1_u) - X\,^1\Sigma_g^+(0_g^+)$, the upper state being the lowest excited state of Ar_2 (see Fig. 1).

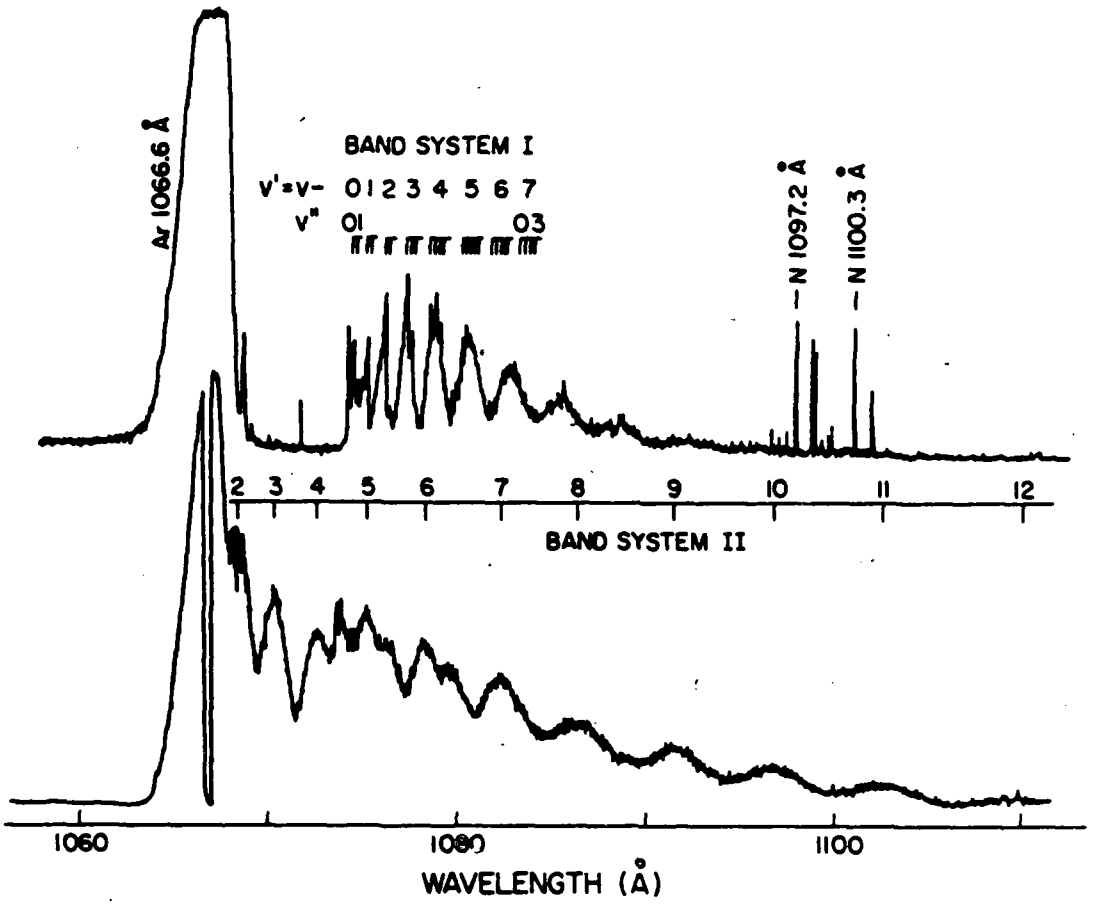

FIG. 3. Densitometer traces of the emission spectrum of argon dimer, band systems I and II. Both spectra are photographed with a 6.65 m spectrograph equipped with 1200 lines/mm grating, in first order, using liquid nitrogen cooled sample, excited with Tesla coil discharge, Kodak 105-05 emulsion type plate. The conditions are: top, $p(\mathrm{Ar}) = 1 + p(\mathrm{He}) = 20$ torr, 15μ slit width 60 min exposure time; bottom, $p(\mathrm{Ar}) = 15$ torr, 15μ slit width, 8 min exposure time. At the bottom curve resonance line of Ar I can be seen as self-reversed.

TABLE I. Band system I, band groups measured at their estimated peaks.[a]

Group No. n	v'	λ(Å)	I[b]	ν(cm^{-1})	Δν	No. of discrete bands
1	$v+1$[c]	1073.5	8	93162	35	2
2	v	1073.8	7	93127	51	3
3	$v-1$	1074.4	7	93075	86	1
4	-2	1075.4	9	92989	113	3
5	-3	1076.7	10	92876	129	4
6	-4	1078.2	9	92747	154	5
7	-5	1080.0	8	92593	189	5 and a diffuse band
8	-6	1082.2	5	92404	221	5 and a diffuse band
9	-7	1084.8	4	92183	288	3 and a diffuse band
10	-8	1088.2	3	91895	312	0 and a diffuse band
11	-9	1091.9	3	91583	359	0 and a diffuse band
12	-10	1096.3	2	91216	414	0 and a diffuse band
13	-11	1101.3	2	90802	443	0 and a diffuse band
14	-12	1106.7	2	90359	479	0 and a diffuse band
15	-13	1112.6	1	89880	554	0 and a diffuse band
16	-14	1119.5	1	89326	650	0 and a diffuse band
17	-15	1127.7	0[c]	88676		0 and a diffuse band

[a]Band groups photographed with 2 m spectrograph in the first order.
[b]Estimated relative intensity within the system. The group No. 5 is given a reference value of 10, the strongest.
[c]The highest upper vibrational level observed but absolute value is unknown. This band has been observed in absorption previously[12(b)] but ignored in classification.

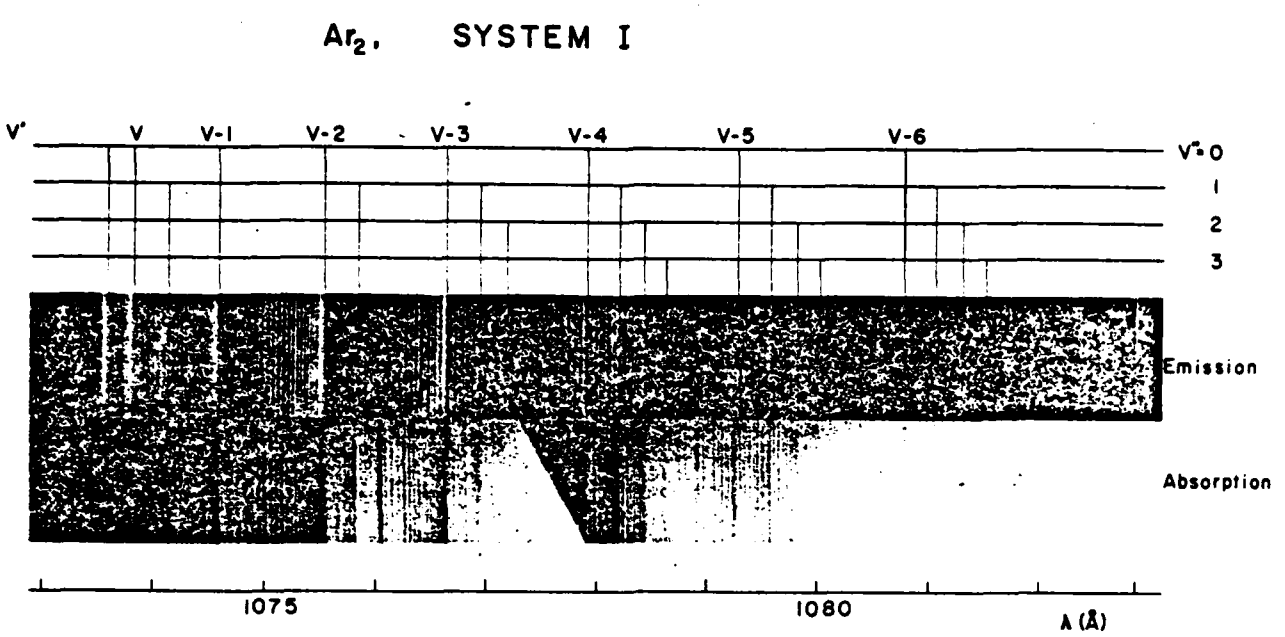

FIG. 4. Discrete bands belonging to band system I. The top spectrum is in emission (white) taken with a 6.65 m spectragraph with a 2400 lines/mm grating used in second order under the conditions; $p(\mathrm{Ar})=2+p(\mathrm{He})=20$ torr, liquid nitrogen cooled, excited with Tesla coil discharge, 15μ slit width, and 60 min exposure time. The bottom spectrum is in absorption (black) taken with the same spectrograph in the same order using; $p(\mathrm{Ar})=15$ torr, 60 min exposure time, cooled with liquid nitrogen, and the argon continuum as background [see Ref. 12(b)]. Note, the classification of strong emission (and absorption) band at 1073.59 Å should read $v'=v+1$, $v''=1$ (see Sec. III.B).

Figure 5 is a densitometer trace of an emission spectrum of the band system I taken under conditions similar to those of the top spectrum in Fig. 4. In the figure one may notice a diffuse band near the long wavelength end of a v'' progression with $v'=v-5$ (band group 7 at 1080 Å) and another one at similar location in the next v'' progression with $v'=v-6$ (band group 8 at 1082 Å). Each of these diffuse bands is structureless and represents a dissociation continuum in emission[29] produced by a transition from an upper vibrational level near its classical turning point on the attractive branch of the potential curve to the ground state at or near its dissociation limit. These diffuse bands are relatively strong and narrow for those associated with the early band groups (No. 7, 8, 9) but become weaker and wider as they progress toward long wavelength; they form an oscillatory (or wavy) spectrum as a whole. An estimate of the observed total band width of the diffuse bands is roughly 180 cm^{-1} for No. 7 the narrowest and 400 cm^{-1} for No. 17 the widest, and others fall orderly in between these two. Energy differences of the consecutive band groups are plotted against the group number n (see Table I) in Fig. 6. In the figure, curve A shows that its slope for $n=1-6$ is nearly the same as that of curve B which is prepared from the $\Delta G(v'+\frac{1}{2})$ value obtained from Table II. Curve A shows a sudden upward bend at $n=7$ and be-

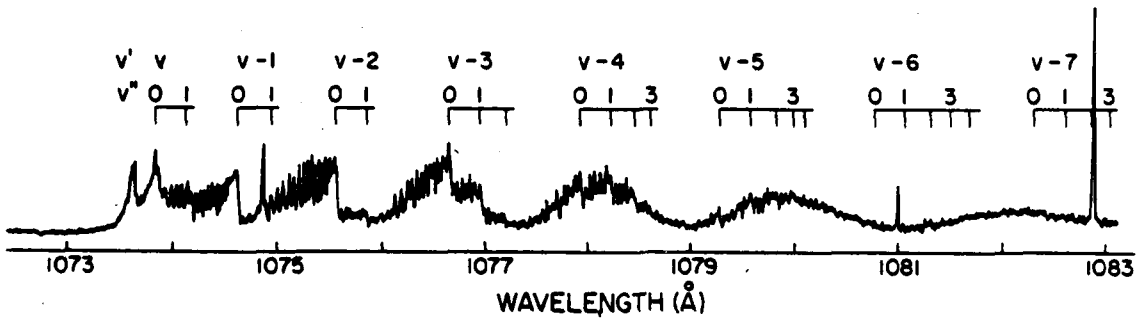

FIG. 5. Densitometer trace of discrete emission bands of the band system I. The original plate was taken with the same spectrograph under experimental conditions similar to that of the top spectrum in Fig. 4. The strong narrow emission peak at the shortest wavelength (1073.59 Å) should be classified as $v'=v+1$, $v''=1$, according to the present work. Three atomic lines are Cu reference lines at 2149.660, 2161.993, and 2165.773 Å (in vacuum).

TABLE II. Band system I, measurements of the band heads.[a]

Group No. n	v', v''	λ(Å)	I^c	ν(cm^{-1})	λ(Å) Absorption[d]	I
1	$v+1^b, 0$	1073.22[e]	1	93177.5_4		
	1	1073.59[e]	8	93145.4_3		
2	$v\ \ ,0$	1073.81	7	93126.3_4	1073.835	10
	1	1074.12	4	93099.4_7	1074.126	5
	2	1074.32	3	93082.1_4		
3	$v-1, 0$	1074.57	7	93060.4_8	1074.604	9
	1	(1074.92)	0		1074.920	3
4	$v-2, 0$	1075.53	9	92977.4_2	1075.548	9
	1	1075.85	3	92949.7_6	1075.838	3
	2	1076.10	2	92928.1_7	1076.076	2
5	$v-3, 0$	1076.63	10	92882.4_2	1076.658	8
	1	1076.95	6	92854.8_2	1076.959	4
	2	1077.17	3	92835.8_6	1077.175	5
	3	1077.36	2	92819.4_6	not observed	
6	$v-4, 0$	1077.92	6	92771.0_6	1077.910	6
	1	1078.20	7	92747.1_7	1078.207	4
	2	1078.47	5	92723.9_5	1078.453	3
	3	1078.60	4	92712.7_8	1078.630	1
	4	1078.78	3	92697.3_1	not observed	
7	$v-5, 0$	1079.26	4	92656.0_8	1079.278	4
	1	1079.58	5	92628.8_1	1079.586	4
	2	1079.82	5	92608.0_3	1079.830	3
	3	1080.00	4	92592.5_9	1080.016	1
	4	1080.11	2	92583.1_6	1080.127	1
8	$v-6, 0$	1080.80	1	92524.0_6	1080.791	2
	1	1081.04	2	92503.5_2	1081.076	3
	2	1081.31	2	92480.4_2	1081.323	2
	3	1081.50	2	92464.1_7	1081.479	1
	4	1081.63	1	92453.0_6	1081.611	1
9	$v-7, 0$	not observed			1082.230	1
	1	1082.60	0[f]	92370.2_2	1082.640	2
	2	1082.90	1	92344.6_3	1082.880	2
	3	1083.10	1	92327.5_8	1083.080	1

[a]Discrete bands photographed with 6.65 m spectrograph in the second order.
[b]The highest upper vibrational level observed. To avoid confusion, v indicates the same vibrational level as in Table I in Ref. 12(b), which means that the vibrational level v is the second highest level observed in the $^3\Sigma_u^+(1_u)$ state.
[c]Estimated relative intensity within the band system. The band $(v-3,\ 0)$ is a given a reference value of 10, the strongest.
[d]Reproduction of the previous absorption data[12(b)] for comparison purpose.
[e]These two bands were not included in system I in our previous work in absorption. They are observed in emission and classified as shown.

comes slightly steeper. The measurement of the peak of the band groups was more accurate for the earlier members up to $n=7$ than that for the late members which are diffuse; this could be the cause for the sudden change in the slope.

A close inspection of Fig. 4 reveals that the $(v, 1)$ and $(v-1, 0)$ bands have more lines in absorption than in emission. These bands are located in the region where system II bands were not thoroughly studied in the previous work[12(b)] and hence there is a good possibility that these excess lines in the absorption spectrum belong to band system II. The top spectrum in the figure has been taken under conditions where system II bands are strongly suppressed (see Sec. III A) so that the system I bands in emission should not be contaminated by those of system II. As will be described later no discrete band was observed in system II in emission.

The band group No. 1 consists of two bands as shown in Table II. These are both newly classified in this work using the same upper vibrational quantum number v as assigned in our previous work.[12(b)] The band at 1073.59 Å is strong but narrow yet indicates a trend of degradation toward short wavelengths with tightly spaced but resolved rotational structures. The band at 1073.22 Å is much weaker and it is difficult to see any resolved structure in it. The former band has been observed in absorption but because of its diffuse appearance [see Fig.

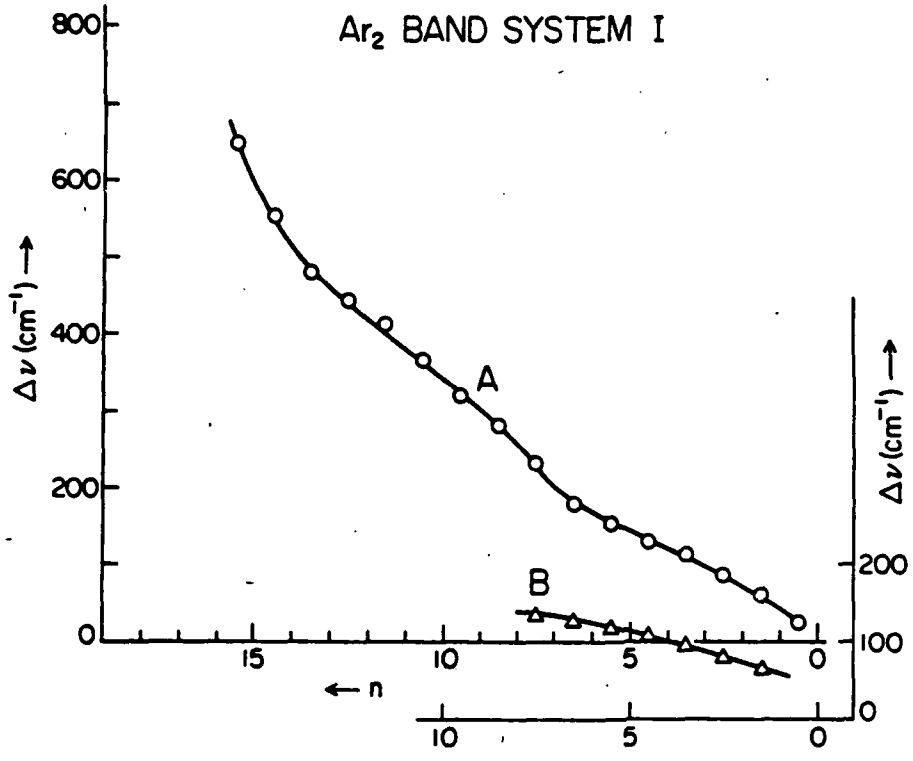

FIG. 6. $\Delta\nu$ vs n curve of band system I. Curve B is drawn using $\Delta G(v'+\frac{1}{2})$ values obtained from the absorption spectrum analysis [see Table II and Ref. 12(b)]. Curve A is drawn using data obtained from spectra taken with the 2 m spectrograph. Peak values for the discrete band groups, $n = 1-7$ in Table I, are estimated from the spectrum.

3, Ref. 12(b)] it was not classified as belonging either to system I or to any other band system of Ar_2. The energy at the highest observed vibrational level, $v' = v+1$ of the upper state of system I is less than that of the separated atom limit, Ar, $3p^6\,{}^1S_0 + Ar^*$, $3p^5(^2P_{3/2})^0 4s$, $J=2$, by 46.2 cm^{-1}.[30] The narrow band width of the 1073.59 Å band is most likely caused by rotational predissociation.[31] A rotational analysis of band system I in emission is in progress at this time and the results will be published in the near future.

It is interesting to note that in Fig. 4 the mutual band intensity distribution within a given v'' progression in the emission spectrum is nearly the same as that for the corresponding progression in the absorption spectrum. In emission this intensity distribution is governed solely by the appropriate Franck–Condon factor; in absorption the same Franck–Condon factors are operative and, since all the relevant v'' levels are comparably populated even at 77 °K, it follows that the band intensity distribution within a given v'' progression will be almost identical in emission and absorption.

C. Band system II

According to the absorption study, band system II originates in the transition $A4s\,{}^1\Sigma_u^+(O_u^+) - X\,{}^1\Sigma_g^+(O_g^+)$, the upper state being the second lowest excited state of Ar_2 (see Fig. 1). In emission this band system seems to consist of two parts, one an oscillatory spectrum composed of 22 diffuse bands and the other the so called second continuum[4]; together they cover a range from 1067 Å to about 1400 or 1500 Å depending upon experimental circumstances. The spectrum excited by a Tesla coil discharge and photographed with the 2 m spectrograph (600 lines/mm grating in first order) is reproduced in Fig. 7. Locations of individual oscillatory peaks are given in Table III. The estimated total band width is in the range from 80 cm^{-1} for band No. 1, the narrowest, to 730 cm^{-1} for No. 22, the broadest of all. The strongest peaks, seen in Fig. 2 and Table III, are Nos. 1 and 2 bands. The peak strength diminishes monotonically toward No. 19 at 1184.3 Å but beyond this point it becomes stronger again due perhaps to superposition of extended part of the second continuum. Densitometer traces of this band system are shown in Fig. 8. The intensity peak of the second continuum is at 1270 ± 2 Å which agrees with the previous measurement.[5]

A puzzling result observed in this band system is that in absorption the spectrum showed at least six strong discrete band groups in the 1066–1074 Å range each of which consisted of two to six well-defined and short wavelength degraded sharp bands. Whereas, in the present work, we are unable to produce these discrete bands in emission and instead, in the same region, we observed four diffuse emission bands which are the No. 1–4 bands in Fig. 2 (see also Table III). We have no reliable explanation for this result at this time but nevertheless, the observed spectrum, which includes the 22 diffuse bands and the second continuum, is classified as band system II for the following three reasons: (1) The observed spectrum occupies the wavelength region where system II can be expected to appear; (2) the intensity of the observed spectrum is stronger than that of system I;

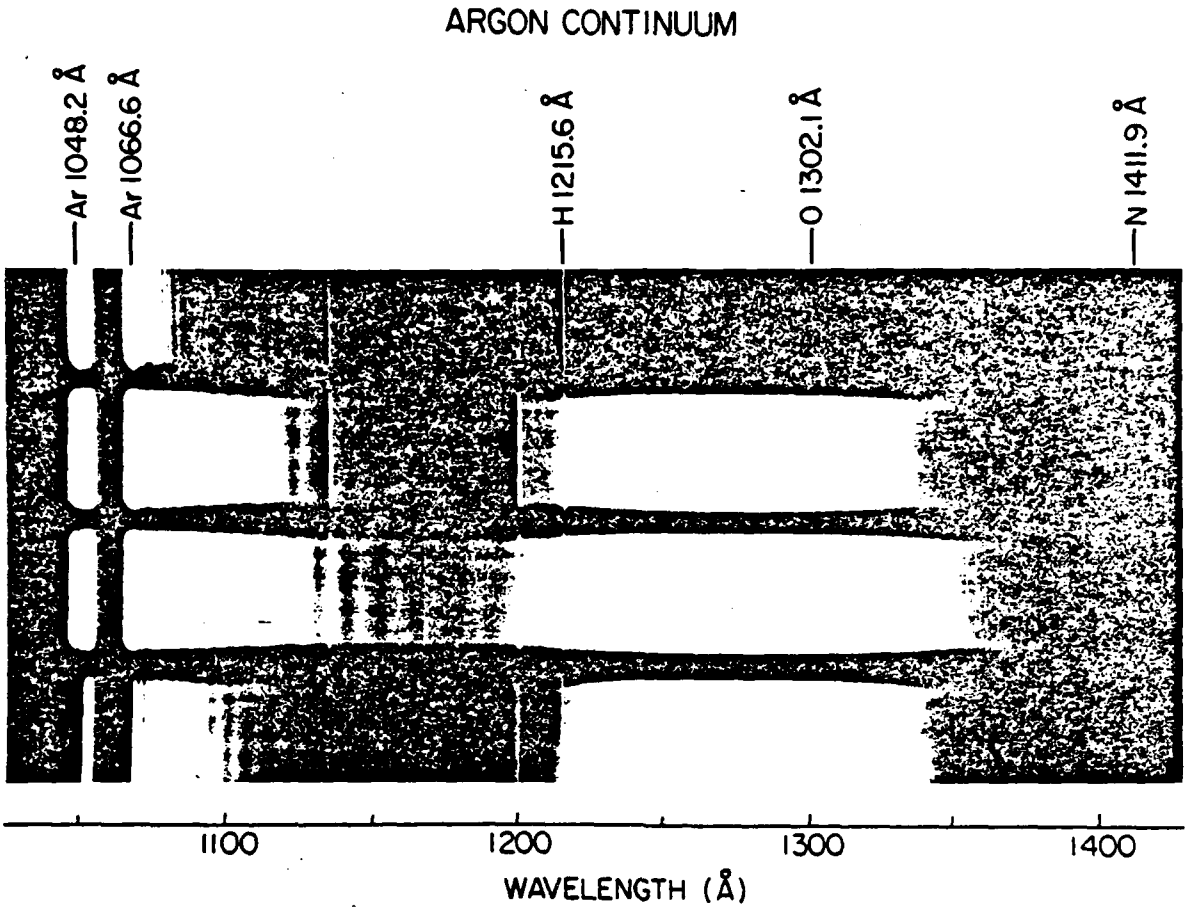

FIG. 7. Emission spectrum of argon dimer in the 1040–1400 Å region. The spectra are photographed using a 2 m spectrograph equipped with 600 lines/mm grating, in first order. The argon pressures used are 2, 5, 10, and 20 torr from top to bottom. Other experimental conditions are: 20μ slit width, 30 min exposure time, sample cooled with liquid nitrogen and excited with Tesla coil discharge. Notice the spectral intensity begins to be weakened at the bottom exposure and that system II (oscillatory spectrum) can be seen strong in the top exposure but the second continuum, peaking at about 1270 Å, is almost absent.

and (3) no other band system is expected in this region other than system II except system I as seen in Fig. 1.

Two tentative explanations of this discrepancy are proposed as follows:

(1) According to our estimate, the internuclear separation of the attractive branch of the upper state potential curve, $4s\,^1\Sigma_u^+(O_u^+)$, of system II (see Fig. 1) at an energy equivalent to that of the argon atom at $3p^5(^2P^0_{3/2})4s$, $J=2$ state [$\equiv 3p^5(^2P^0)4s$, $J=2$, in Fig. 1] will be smaller than $R_e = 3.8$ Å of the ground state curve of Ar_2 by a few tenths of 1 Å and it will be close to $R(D_0^0)$, the internuclear separation where the repulsive branch of the ground state potential curve meets its asymptote [for more detailed curve see Refs. 15, 25(g), (h)]. In this case, the situation strongly suggests that the emission spectrum produced by a transition from the point at the upper state mentioned above to the ground state directly below will produce a discrete band group (v'' progression) in association with a diffuse band, i.e., dissociation–continuum. The diffuse band thus produced is not expected to be weakened by reverse transitions while the discrete bands will be weakened considerably since in absorption the former is very weak while the latter are very strong.[12(b)] As a result, the diffuse bands will remain strong in emission and provide the oscillatory spectrum whereas the discrete bands become weak and possibly can be observed in absorption if there is background radiation available. In fact, we observed five groups of absorption bands in the 1066–1073 Å region with the diffuse bands as background; they are the v'' progressions of band system II with $v' = v+1$, v, $v-1$, $v-2$, and $v-3$, some of these can be seen in top two spectra in Fig. 2. It seems plausible to relate the emission and absorption bands of system II in such a way that the absorption bands ($v' = v+2$, $v'' = 0$) of Ref. 12(b) and the emission band No. 1 in the present Table III are assumed to have $v' = v+2$ as their common upper level. Similarly, we may relate the $(v+1, 0)$ absorption band to the emission band No. 2, and so on. On this basis, the energy difference between a $(v', 0)$ absorption band head and the related emission peak corresponds to the energy

TABLE III. Band system II, measured at intensity peaks.

Band No. n	λ(Å)	I[a]	ν(cm^{-1})	Δν	Remarks
1	1067.3	10	93694	79	This band is superimposed upon the pressure broadened first resonance line of Ar I.
2	1068.2	10	93615	157	
3	1070.0	9	93458	201	
4	1072.3	7	93257	242	
5	1075.1	5	93015	285	Superimposed upon system I, $v' = v-2$, v'' progression.
6	1078.4	5	92730	326	Located between two v'' progressions with $v' = v-4$ and $v-5$ of system I.
7	1082.2	6	92404	365	Coincides with band group No. 8 of system I.
8	1086.5	5	92039	414	
9	1091.4	5	91625	451	Coincides with No. 11 band group of system I
10	1096.8	5	91174	496	Coincides with No. 12 band group of system I.
11	1102.8	4	90678	564	
12	1109.7	4	90114	612	
13	1117.3	4	89502	660	
14	1125.6	3	88842	713	
15	1134.7	3	88129	785	Superimposed upon N I line group at 1134 Å.
16	1144.9	3	87344	876	
17	1156.5	3	86468	976	
18	1169.7	3	85492	1054	
19	1184.3	3	84438	1167	
20	1200.9	4	83271	1304	Superimposed upon N I line group of 1200 Å.
21	1220.0	4	81967	1523	
22	1243.1	5	80444		

[a]Estimated relative intensity within the band system. The strongest bands at 1067.3 and 1068.2 Å are given reference value of 10.

separation between the $v'' = 0$ level and the point on the repulsive wall of the ground state at which the bound-free emission transition terminates. The differences thus obtained are 87.7, 88.9, 154.8, 245.7, 366.5, and 511.9 cm^{-1} for the emission bands No. 1, 2, ..., 6. The lowest two differences are, as would be expected, close to the ground state dissociation energy $D_0^0 = 84$ cm^{-1}, and the subsequent differences show the expected rather rapid increases as the increasingly steep repulsive wall is ascended. The existence of discrete emission in the first two cases may exist, but the observation would be difficult because of obscuration by the broadened argon resonance line.

(2) An alternate explanation is that band system II would be produced by a continuum–continuum transition rather than by a bound–continuum transition such as system I. Mies and Smith[32(a)–(c)] have suggested an extension of the concept of a continuum–continuum transition[33] to explain the diffuse emission spectrum of the helium dimer in the 600–614 Å region in place of the previous one involving a bound–continuum transition.[34,35] In their interpretation the diffuse emission bands of He_2[35] are produced by transitions from a vibrational continuous level, belonging to the $A\,^1\Sigma_u^+$ state and located slightly (several hundred wavenumbers) above its dissociation limit, to the ground state $X\,^1\Sigma_g^+$ which is a continuous state. In this kind of transition, one cannot expect discrete bands and the spectrum will consist of a series of diffuse bands appearing as an oscillatory spectrum as a whole. It should be noted that according to Sando and Dalgarno[36(a)] the first two bands at 600.04 and 601.06 Å observed in absorption[12(a)] arise from transitions into quasibound resonating vibrational levels of the $A\,^1\Sigma_u^+$ state.

If the M–S type, continuum–continuum transition is the case for system II of Ar_2 in emission as suggested above, then it should begin with strong and diffuse bands near the first resonance line of Ar I and extend toward long wavelengths with decreasing intensity. As the internuclear distance of the nodal point decreases further [see Fig. 1, Ref. 32(a)] the band will begin to become stronger again and perhaps broader at the same time.

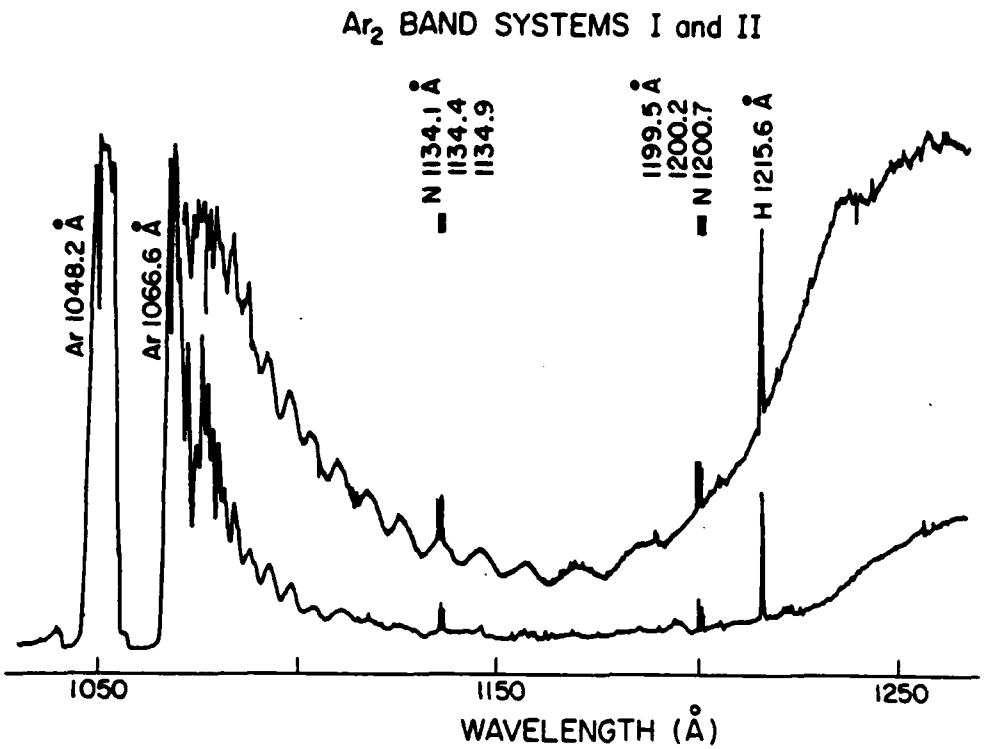

FIG. 8. Densitometer traces of the band system II. Original spectra are taken with the 6.65 m spectrograph in first order. Experimental conditions are for the top trace: $p(Ar) = 15$ torr, cooled with liquid nitrogen, Tesla coil discharge, 30 min exposure time; for the bottom trace: $p(Ar) = 6$ torr, liquid nitrogen cooled, Tesla coil discharge, 15 min exposure time. About five times the exposure time is required for the same intensity with an uncooled (room temperature) sample. The discrete bands of system I are superimposed in the range 1073.5 ~ 1080.0 Å.

A band produced by a transition from the last nodal point to the ground state would be quite wide and strong. The spectrum thus expected in the M–S type continuum–continuum transition for band system II seems to agree qualitatively with the results shown in Figs. 7 and 8. However, according to Mies and Smith, a deep potential well depth in the upper state, as much as 2.5 eV in the case of the $A\,^1\Sigma_u^+$ state of helium dimer, would be required for a transition of this type. The dissociation energy of the $4s\,^1\Sigma_u^+(O_u^+)$ state of Ar_2 is however only 0.74 ±0.07 eV[39(b)] and accordingly, the second explanation is less likely than the first [see also Ref. 39(b)]. A quantitative investigation is desired for confirmation of either of the two interpretations suggested.

It is significant that a relatively weak excitation such as a nonpulsed transformer discharge or a Tesla coil discharge is essential for the production of a clear oscillatory spectrum of the argon dimer in the vuv region.

D. Band system III

This is the strongest of the three band systems of Ar_2 observed in emission as well as in absorption. Seven bands were observed in this work immediately to the long wavelength side of the second resonance line of Ar I at 1048.2 Å. These are listed in Table IV. The individual bands in the table are all diffuse and do not correspond with the system III absorption bands,[12(b)] nevertheless, these are classified as belonging to the band system III based on the following evidence: (1) The wavelength region where the seven bands are observed is practically the same as the region where the absorption bands were observed. (2) The location of the bands with respect to the resonance line is also practically identical

TABLE IV. Band system III, diffuse bands.[a]

Band No. n	λ(Å)[b]	I[c]	ν(cm^{-1})	$\Delta\nu$	Band[e] width
1	1049.6	100	95274	36	18
2	1050.0	90	95238	73	34
3	1050.8	20	95165	90	49
4	1051.8	5	95075	136	73
5	1053.3	2	94939	162	51
6	1055.1	0[d]	94777	152	20
7	1056.8	0[d]	94625		20

[a]Measured at estimated band center and accurate within ±0.2 Å.
[b]We are convinced that these bands are not grating ghosts of the 1048 Å line of Ar I although the latter line appears extremely strong with variable width of self absorption at the center.
[c]Roughly estimated relative intensity, No. 1 band is given a reference value of 100.
[d]Extremely weak, only observed in one plate photographed with a long exposure time.
[e]Roughly estimated width, accurate within ±10 cm^{-1}.

with that of the first four bands, No. 1–4, of system II with respect to the first resonance line of ArI. (3) Some of the system III bands are observed in absorption as occurs for four diffuse bands, No. 1–4, of system II.

In view of this evidence, these seven diffuse bands should belong to the band system III and most probably are dissociation continua, each of which is associated with an individual band group, v'' progression. A possibility that the transition will be a M–S type continuum–continuum transition cannot be excluded at this point although it is unlikely because the dissociation energy of the upper state is only 423 cm^{-1} (0.05 eV).[12(b)]

It is worthwhile mentioning that a preliminary study of the krypton dimer emission spectrum showed a close similarity with the corresponding band system of Ar_2 reported in this work particularly for system III. The krypton spectrum showed seven diffuse bands appearing in the same region where the absorption bands were observed.[12(d)] The characteristics of the bands and their behavior with respect to pressure variation are also almost identical to that of Ar_2. The results will be reported in the near future.

E. Band system x in the 1110–1160 Å region

When relatively low pressure argon (~4 torr) was excited with a pulsed transformer discharge 15 diffuse bands were observed in the 1111–1157 Å range (see also Table II, Ref. 4). They appear superimposed upon a weak continuum which begins at 1066 Å and extends to about 1160 Å. The diffuse bands are listed in Table V. The individual bands are broad and diffuse yet all show an indication of a degredation toward short wavelengths. No other Ar_2 band systems were observed under the same experimental conditions. If a mixture of argon (~4 torr) and helium (~40 torr) was excited with the same mode of excitation, the band system I of Ar_2 appeared as strong as the present bands and in addition the $(HeAr)^*$ bands at 1445 and 1457 Å[37] also were observed.

One of us (Y.T.) has reported an emission band group of Xe_2 in the 1584–1621 Å region and included, in the same report, five emission bands of system x of Ar_2 (see Table II, Ref. 4). In regard to the xenon bands, Mulliken has suggested[19] that these may represent transition from low vibrational levels of $A6s$, $^1\Sigma_u^+(O_u^+)$ and/or $^3\Sigma_u^+(1_u)$ to the ground state $X\,^1\Sigma_g^+(O_g^+)$. Since these transitions correspond to those of band systems II and I of Ar_2, respectively, and these systems are extensively observed in this work we should expect to find the bands belonging to system x in either system II or I. Comparison of Table V with Tables I and III reveals only two rather weak bands, 1110.6 and 1125.9 Å, are in common. We have no reliable explanation for the absence of other bands of system x in either Table I or III. The work is continuing.

IV. DISCUSSION

The second continuum of Ar_2 with its peak at about 1270 Å[4,5] is produced strongly in a Tesla coil discharge of liquid nitrogen cooled argon and its intensity variation vs argon pressure parallels that of the oscillatory spectrum of band system II. It has been suggested[19] that the second continuum is produced by transitions from the lowest vibrational level of the $^1\Sigma_u^+(O_u^+)$ and/or $^3\Sigma_u^+(1_u)$ state to the ground state, a continuous state with a shallow potential well depth of 98.7 m^{-1}.[14] Thus the transition should be a bound–continuum type and not the M–S type continuum–continuum transition (suggestion 2, Sec. III C). If this is indeed true, the large dimer population at low lying vibrational levels of the excited state required for the strong continuum would have to be supplied by other processes in addition to that usually assumed, i.e., the recombination of an excited argon atom at $4s(3/2)J=1$ with a normal atom at high vibrational levels of the $^1\Sigma_u^+(O_u^+)$ or $^3\Sigma_u^+(1_u)$ state followed by collisional relaxation to low levels. One of the candidates for this will be molecular excitation directly from the ground state to the low vibrational levels of the upper state by electron impact, although the Franck–Condon factor diminishes rapidly toward lower vibrational levels in the upper state. The intensity enhancement of the continuum on cooling the sample with liquid nitrogen supports a mechanism involving ground state dimers. A cascade transition from a highly excited state of Ar_2^* (or from Ar_2^+) to low vibrational levels of the $^1\Sigma_u^+(O_u^+)$ state is another candidate though no adequate spectroscopic evidence to support this was observed in this work.

The origin of the so called first continuum of Ar_2[4,5] is not clear at this time. Three band systems, I, II, x, and one continuum, which is superimposed upon the x system, appear in the same range 1066–1150 Å as the first continuum. The spectral characteristics of these differ and their appearance depends very much upon the mode of excitation as well as experimental conditions. Thus, in our opinion, any one or a combination of these can become the first continuum. Most likely the first continuum of argon observed and so designated by one of us[4] will be primarily a broadened oscillatory spectrum of band systems I & II. Thonnard and Hurst's 1100 Å continuum[38(a)] may originate by a combination of system

TABLE V. Band system x, diffuse bands.[a]

Band No. n	λ(Å)	I^b	ν(cm^{-1})	$\Delta\nu$
1	1110.6	3	90041	636
2	1118.5	10	89405	239
3	1121.5	3	89166	127
4	1123.1	3	89039	222
5	1125.9	4	88817	240
6	1127.6	4	88683	110
7	1129.0	2	88573	530
8	1135.8	2	88043	178
9	1138.1	8	87865	261
10	1141.5	6	87604	177
11	1143.8	1	87427	274
12	1147.4	3	87153	121
13	1149.0	2	87032	267
14	1151.2	1	86865	435
15	1157.0	0*	86430	

[a]Measured at estimated band head and accurate within ± 0.2 Å.
[b]Estimated relative intensity within the band system. The band at 1118.5 Å is given a reference value of 10, the strongest.

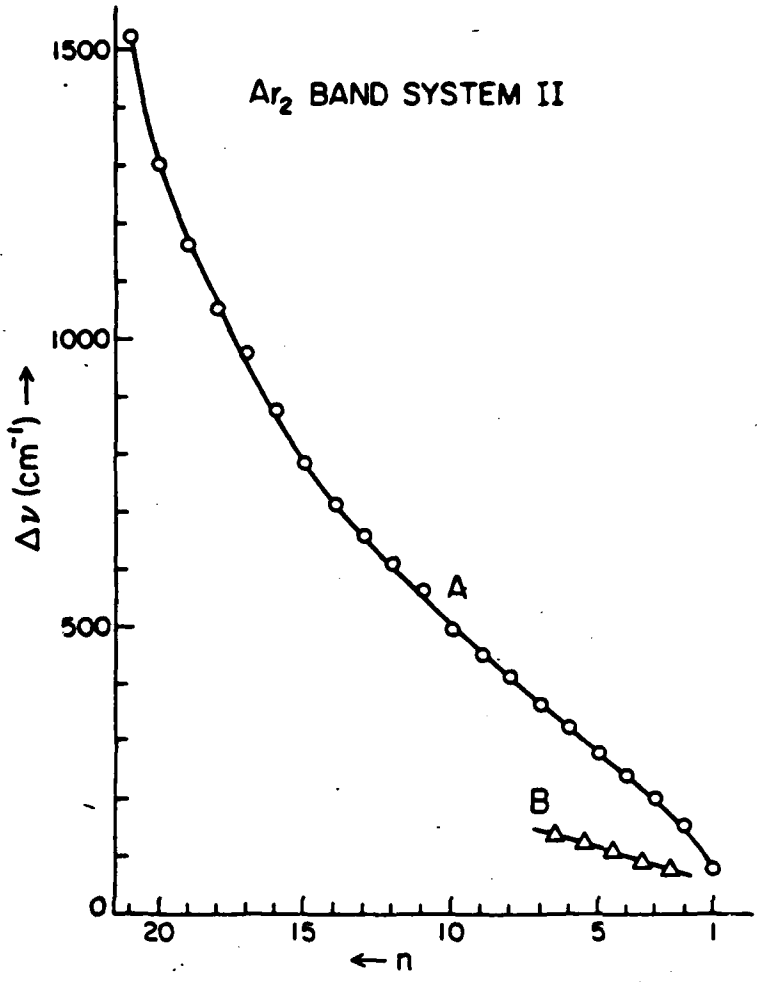

FIG. 9. $\Delta\nu$ vs n curves of the band system II. Curve B is drawn using $\Delta G(v'+\frac{1}{2})$ values obtained from the absorption spectrum [Ref. 12(b)] but curve A is drawn using the present data obtained from the spectrum photographed with the 2 m spectrograph. n indicates the group number appearing in Table III.

x and a continuum superimposed upon it. Michaelson and Smith[39(b)] observed a continuous spectrum in their afterglow experiment which begins at 1074 Å and called it the first continuum. The presently observed three strong band groups No. 1, 2, and 3 of system I probably contribute to their first continuum because these are located at the right location and appear strong even when argon alone was excited in the Tesla coil discharge as seen in the top two spectra in Fig. 2. Michaelson and Smith[39(a)] observed an argon atomic line which corresponds to the forbidden line at 1073.6 Å of the transition $3p^5(^2P^0_{3/2})4s$, $J=2 \rightarrow 3s^23p^6\,^1S_0$. In the present work we were unable to observe this line either in emission or in absorption and instead a narrow and sharp band with resolved rotational structures was observed at the same place in both emission and absorption (see Fig. 4 and Table II). It is interesting to note that a continuum like spectrum similar to Michaelson and Smiths' first continuum at 1074 Å was reported in a previous paper (see Fig. 3, Ref. 40).

The positions of intensity peaks in the oscillatory structure measured and classified by Michaelson and Smith as system II agree with the present value for the same band system with a few exceptions [see Table II, Ref. 39(b), and Table III of this work]. The principal reason for their classification of the oscillatory spectrum as belonging to the band system II is that the vibrational spacing vs $E(v)$ plots for their spectrum clearly showed that $Ar^* 3p^5(^2P^0_{3/2})4s$, $J=2 \rightarrow Ar$, $^1S_0$ cannot be the dissociation product of the upper state. This conclusion came from a comparison of the plots with similar plots for the upper states of band systems I and II known in absorption. The energy intervals of successive peaks of the oscillatory spectrum are plotted vs n, the group number, for system II and shown in Fig. 9. The curve A in Figs. 6 and 9 has a similar trend except that the curve in the latter is steeper than that in the former at small n (1 ~ 5) where the spectrum showed no discrete bands. Our present study does not lead to an appreciable improvement over their potential curve and its dissociation energy for the upper state $4s\,^1\Sigma_u^+(O_u^+)$. Thus the most reliable dissociation energies available at this time would be $D_e = 0.74 \pm 0.07$ eV for the $4s\,^1\Sigma_u^+$[39(b)] and $D_e = 0.78 \pm 0.4$ eV for $4s\,^3\Sigma_u^+$.[41]

ACKNOWLEDGMENTS

This work was supported by the Air Force Office of Scientific Research under contract AFOSR-77-3137 and AFOSR-77-3137A. Part of this work was carried out

at Air Force Geophysics Laboratory. We are grateful to members of the Laboratory for their help.

The authors are thankful to Dr. D. C. Lorents and Dr. R. E. Olson for their permission to use their potential curves of argon dimer.

[1]J. J. Hopfield, Astrophys. J. 72, 133 (1930).
[2]Y. Tanaka and M. Zelikoff, J. Opt. Soc. Am. 44, 254 (1954).
[3]P. G. Wilkinson and Y. Tanaka, J. Opt. Soc. Am. 45, 344 (1955).
[4]Y. Tanaka, J. Opt. Soc. Am. 45, 710 (1955).
[5]R. E. Huffman, Y. Tanaka, and J. C. Larrabee, Appl. Opt. 2, 617 (1963). (See references in this article for more references up to 1963.)
[6]R. E. Huffman, J. C. Larrabbe, and Y. Tanaka, Appl. Opt. 4, 1581 (1965).
[7]P. G. Wilkinson, Can. J. Phys. 45, 1715 (1967).
[8]P. E. Siska, J. M. Parson, and Y. T. Lee, J. Chem. Phys. 55, 5762 (1971).
[9]J. M. Parson, P. E. Siska, and Y. T. Lee, J. Chem. Phys. 56, 1511 (1972).
[10]C. H. Chen, P. E. Siska, and Y. T. Lee, J. Chem. Phys. 59, 601 (1973).
[11]J. A. Barker, R. O. Watts, J. K. Lee, T. P. Schafer, and Y. T. Lee, J. Chem. Phys. 61, 3081 (1973).
[12](a) Y. Tanaka and K. Yoshino, J. Chem. Phys. 50, 3087 (1969); (b) 53, 2012 (1970); (c) 57, 2964 (1972); (d) Y. Tanaka, K. Yoshino, and D. E. Freeman, *ibid.* 59, 5160; (1973). (e) D. E. Freeman, K. Yoshino, and Y. Tanaka, *ibid.* 61, 4880 (1974).
[13]M. C. Castex, Chem. Phys. 5, 448 (1974).
[14]R. J. LeRoy, J. Chem. Phys. 57, 573 (1972).
[15]E. A. Colbourn and A. E. Douglas, J. Chem. Phys. 65, 1741 (1976).
[16]N. Bérnardes and H. Primakoff, J. Chem. Phys. 30, 691 (1959).
[17]D. D. Konowalow and S. Carra, Phys. Fluids 8, 1585 (1965).
[18]J. A. Barker and A. Pompe, Aust. J. Chem. 21, 1683 (1968).
[19]R. S. Mulliken, J. Chem. Phys. 52, 5170 (1970).
[20]H. J. M. Hanley, J. A. Barker, J. M. Parson, Y. T. Lee, and M. Klein, Mol. Phys. 24, 11 (1972).
[21](a) R. G. Gordon and Y. S. Kim, J. Chem. Phys. 56, 3122 (1972); (b) 56, 2801 (1972); (c) C. Starkschell and R. G. Gordon, *ibid.* 57, 3213 (1972).
[22]K. K. Docken and T. P. Schafer, J. Mol. Spectrosc. 46, 451 (1973).
[23]D. D. Konowalow and D. S. Zakheim, J. Chem. Phys. 57, 4375 (1972).
[24]T. L. Barr, Diana Dee, and F. R. Gilmore, J. Quantum Spectrosc. Radiat. Transfer 15, 625(1975).
[25]For detailed information see references included in the following articles, for example: (a) J. O. Hirschfelder, C. F. Curtiss, and R. B. Bird, *Molecular Theory of Gases and Liquids* (Wiley, New York, 1954); (b) E. A. Guggenheim and M. L. McGlashen, Proc. R. Soc. (London) A 255, 456 (1960); (c) R. J. Munn, J. Chem. Phys. 40, 1439 (1964); (d) R. C. Leckenby and E. J. Robbins, Proc. R. Soc. (London) A 291, 389 (1966); (e) F. T. Greene and T. A. Milne, J. Chem. Phys. 39, 3150 (1963); (f) 47, 4095 (1967); (g) L. W. Bruch and I. J. McGee, *ibid.* 53, 4711 (1970); (h) J. A. Barker, R. A. Fisher, and R. O. Watts, Mol. Phys. 21, 657 (1971).
[26]The differential pumping system was available only for the 6.65 m spectrograph.
[27]D. C. Lorents and R. E. Olson, Technical Report No. 1 for the Office of Naval Research, Contract N000 14-72-C-0457. NRL Reg-00173-2-006435/4-19-72. EAM Stanford Research Institute, Dec. 27, 1972. See also D. C. Lorents, Physica (Utrecht) 82C, 19 (1976).
[28]For atomic state designation see: C. E. Moore, Atomic Energy Levels, Circ. U. S. Natl. Bur. Stand. 467, Vol. 1, 212 (1949).
[29]Term "dissociation continuum" has been primarily defined in absorption spectroscopy. Since the evidence observed here has similarities with the absorption we used the same terminology. See G. Herzberg, *Spectra of Diatomic Molecules* (Van Nostrand, New York, 1950), pp. 388–405.
[30]This value is obtained from D_0^0 of the ground state by LeRoy (Ref. 14) and the energy of the $3p^5 4s(3/2)^0 J = 2$ level of Ar I (Ref. 28).
[31]See Ref. 29, pp. 413–425.
[32](a) F. H. Mies and A. L. Smith, J. Chem. Phys. 45, 994 (1966); (b) A. L. Smith, *ibid.* 47, 1561 (1967); (c) F. H. Mies, *ibid.* 48, 482 (1968); (d) A. L. Smith, *ibid.* 49, 4817 (1968); (e) K. W. Chow, A. L. Smith, and M. G. Waggoner, *ibid.* 58, 4208 (1971); (f) K. W. Chow and A. L. Smith, *ibid.* 54, 1556 (1971).
[33]See for example, Ref. 29, p. 394.
[34]J. Nickerson, Phys. Rev. 47, 707 (1935).
[35]Y. Tanaka and K. Yoshino, J. Chem. Phys. 39, 3081 (1963).
[36](a) K. M. Sando and A. Dalgarno, Mol. Phys. 20, 103 (1971); (b) K. M. Sando, *ibid.* 21, 439 (1971); (c) 23, 413 (1972).
[37]Y. Tanaka, K. Yoshino, and D. E. Freeman, J. Chem. Phys. 62, 4484 (1975).
[38](a) N. Thonnard and G. S. Hurst, Phys. Rev. A 5, 1100 (1972); (b) G. S. Hurst, T. E. Bortner, and T. D. Strickler, Phys. Rev. 178, 4 (1969).
[39](a) R. C. Michaelson and A. L. Smith, Chem. Phys. Lett. 6, 2 (1970); (b) R. C. Michaelson and A. L. Smith, J. Chem. Phys. 61, 2566 (1974).
[40]R. E. Huffman, Y. Tanaka, and J. C. Larrabee, Jpn. J. Appl. Phys. 4, 494 (1965).
[41]K. T. Gillen, R. P. Saxon, D. C. Lorents, G. E. Ice, and R. E. Olson, J. Chem. Phys. 64, 1925 (1976).

Emission spectrum of rare gas dimers in the vacuum UV region. II. Rotational analysis of band system I of Ar_2

D. E. Freeman and K. Yoshino

Harvard-Smithsonian Center for Astrophysics, Cambridge, Massachusetts 02138

Y. Tanaka

Quantum Institute, University of California, Santa Barbara, California 93106

(Received 10 April 1979; accepted 9 May 1979)

The emission spectrum of Ar_2 excited by a Tesla discharge has been photographed at high resolution in the region 1073.5–1081.5 Å by 6.65 m spectrograph. Experimental conditions were chosen to produce only the band system emitted in the transition from the lowest excited state to the ground state. Rotational analyses of several bands indicate that the coupling scheme in the lowest excited state is closer to Hund–Mulliken case *b* than to case *c*, so that the excited state symmetry may be assigned approximately as $^1\Sigma_u^+$ rather than $1_u, 0_u^-$. Rotational constants obtained for seven high-lying emitting levels with consecutively decreasing vibrational quantum numbers range from 0.073 to 0.105 cm^{-1}. An attempt has been made to use spectroscopic results to depict the shapes and positions of the long range portions of the potential curves of the first two excited states ($^3\Sigma_u^+$ and $^1\Sigma_u^+$) of Ar_2 relative to each other and to that of the ground state $X\,^1\Sigma_g^+$.

I. INTRODUCTION

Current interest in the ground and excited states of the diatomic rare gas molecules has been stimulated as a result of the possibility of developing high intensity vacuum ultraviolet (VUV) lasers based on the bound–free excimer transitions in these systems,[1,2] and such lasing has been demonstrated for argon.[2] The lower excimer states of the rare gases are also important because the electronic energy stored in them as an end result of electron–beam excitation can be transferred to another rare gas[3] or to various minor added constituents from which significant visible and near UV emissions have been observed.[4] The lowest excimer state of a rare gas molecule, being relatively long lived, is an especially important energy reservoir, and the amount of electronic energy available for transfer remains large even if the excimer is vibrationally relaxed. Information relating to the potential energy curves of the diatomic rare gas molecules obtained from absorption and emission spectroscopy, molecular beam scattering experiments, and theoretical calculations can be found among the references cited in three recent papers.[5–7]

In the most recent spectroscopic work on the VUV absorption spectrum of Ar_2, Colbourn and Douglas[5] re-examined the nine groups of absorption bands previously observed at somewhat lower resolution.[8] They found that, even at a reciprocal dispersion of 0.24 Å/mm, only one of these band systems, viz., System II, which is located in the region 1068–1074 Å, showed rotational structure that could be analyzed with confidence. The information extracted from this rotational analysis was used to obtain a refined potential curve and energy levels for the $^1\Sigma_g^+(0_g^+)$ ground state of Ar_2 in the region of its van der Waals bowl, to evaluate some spectroscopic constants of the second excited electronic state $^1\Sigma_u^+(0_u^+)$ of Ar_2, which is derived from the separated atom limit Ar, $3p^6\,^1S_0 + Ar^*$, $4s(3/2)_1^0$, and to confirm the assignment[8] of the absorption System II as $^1\Sigma_u^+(0_u^+) - X\,^1\Sigma_g^+(0_g^+)$.

In recent spectroscopic work on the VUV emission spectrum of Ar_2, Tanaka, Walker, and Yoshino[7] describe four band systems in the 1000–1500 Å region, all of which were found to terminate on the ground state $X\,^1\Sigma_g^+(0_g^+)$ of Ar_2. In the present paper some of the emission bands of System I, viz., those in the region 1073–1082 Å, are rotationally analyzed, and new information is presented on the angular momentum coupling scheme (electronic symmetry) and spectroscopic constants of the lowest excited electronic state of Ar_2 which is derived from Ar, $3p^6\,^1S_0 + Ar^*$, $4s(3/2)_2^0$.

II. EXPERIMENTAL

The general conditions under which the emission spectrum of Ar_2 is excited by a Tesla discharge have already been described,[7] and only the specific experimental details relevant to obtaining the spectra at high resolution will be given here. A 6.65 m McPherson vacuum spectrograph equipped with a platinum coated 2400 line/mm ruled grating is used and provides a reciprical dispersion of 0.30 Å/mm in the second order. The argon or argon–helium mixture flows through a windowless cell to which the Tesla discharge is applied. The central 20 cm of this 30 cm cell is cooled by liquid nitrogen, and the discharge is restricted to the cooled section. A small fraction of the argon or argon–helium mixture from the cell enters the spectrograph through the slit, immediately behind which is a differential pumping system. Cu I and Cu II lines in the first order from a hollow cathode lamp are used as standards for the argon spectra photographed in the second order on Eastman Kodak 101-05 plates. Exposure times are typically 60 min with a 15 μ slitwidth. Wavelength measurements of sharp lines are estimated to be accurate to ±2 mÅ. In the argon–helium mixtures used to obtain the best emission spectra the argon pressure ranged from 3 to 8 Torr and the helium pressure from 14 to 36 Torr.

III. RESULTS

A. General

Since the emission band system I (1073–1128 Å) and band system II (1067–1243 Å) occupy almost the same

 0021-9606/79/161780-14$01.00

wavelength region, we exploit a technique employed by Tanaka *et al.*[7] which suppresses or eliminates system II and leaves system I isolated. This technique consists in using not argon alone in the discharge cell, but a mixture of argon with excess helium. The effectiveness of this means of observing system I in isolation from system II is well illustrated in Figs. 2 and 3 of Ref. 7. Seventeen band groups were observed in band system I (Table I, Ref. 7), but of these only nine with peak intensities in the region 1073.5–1084.8 Å possess any discrete bands.

The ground state vibrational numbering v'' of levels was established previously[8] for the discrete absorption bands of system I, and the v'' numbering of the discrete emission bands is established by comparison of the emission and absorption band heads listed in Table II of Ref. 7. The absolute numbering for the upper state vibrational levels giving rise to discrete emission bands in system I is unknown, and we adopt the same arbitrary notation as given in Table II of Ref. 7, i.e., the v' levels are labeled in consecutively decreasing order from $v'=v+1$ for the highest v' level through $v'=v-7$ for the lowest v' level giving rise to discrete (v', v'') bands.

We performed rotational analyses, with varying degrees of completeness, for bands with $v'=v$ through $v'=v-6$. Even in the absence of system II, the general appearance of system I in emission is, with the apparent exception of the $(v-2, 0)$ band, that of a spectrum consisting mainly of overlapping branches. All of the observed emission bands are shaded towards short wavelengths with their heads at the long wavelength edges.

B. Electronic assignment of the lowest excited state of Ar_2

The emission spectrum to the ground state of Ar_2 from the lowest excited molecular state derived from the separated atom limits Ar^*, $4s(3/2)_2^0 + Ar$, $3p^6\,{}^1S_0$ may be assigned as 0_u^-, 1_u (case c) $- X0_g^+$ or ${}^3\Sigma_u^+$ (case b) $- X\,{}^1\Sigma_g^+$, and the transition between cases b and c is discussed by Herzberg.[9] For case c, the $0_u^- - X0_g^+$ component is forbidden and the electric dipole allowed component $1_u - X0_g^+$ would give rotational structure consisting of three branches (R, Q, and P), rather similar to the structure arising from a ${}^1\Pi - {}^1\Sigma$ transition. For case b, ${}^3\Sigma_u^+ - X\,{}^1\Sigma_g^+$, which is spin forbidden, four rotational branches ${}^RR$, ${}^PP$, ${}^RQ$, and ${}^PQ$ are expected to be observed[8,10] and to have comparable intensities except at very low J values[11]; the differences $({}^RR - {}^RQ)$ and $({}^PP - {}^PQ)$ depend only on the spin splittings in the upper state. If these differences were not resolved experimentally then we should expect essentially two branches ${}^RR$ and ${}^PP$ which would behave like ordinary R and P branches. If the coupling scheme in upper state of system I were approximately case b, ${}^3\Sigma_u^+$ then the usual nonrigid rotor term value formula

$$T_v(J) = G(v) + B_vJ(J+1) - D_vJ^2(J+1)^2 \qquad (1)$$

would be applicable to levels not too close to the dissociation limit.

All the lines that are ${}^PQ$ in pure case b become forbidden (with upper state 0_u^-) in pure case c, whereas all of the ${}^RQ$ lines (except for $J=0$) become allowed Q lines in pure case c. So, if the coupling is closer to case b, and if we observe ${}^RR$ and ${}^RQ$ unresolved and ${}^PP$ and ${}^PQ$ unresolved, we expect the latter pair to lose intensity relative to the former as a result of deviation from pure case b.

In earlier work on the vibrational analysis of system I in absorption,[8] the upper state was considered only in terms of Hund–Mulliken case c coupling, and the assignment 1_u was suggested. Later, Colburn and Douglas[5] concurred with this suggestion, adding briefly that the extensively overlapped absorption bands of system I apparently possessed Q branches. However, they did not examine system I in any detail in their paper, which was devoted primarily to an excellent rotational analysis of system II in absorption. In our preliminary rotational analysis of the $(v-2, 0)$ emission band of system I we found no evidence for the existence of a Q branch. Nor, in extending and elaborating our analysis to other more complicated emission bands of system I, did we find definitive evidence for the existence of Q branches. The weakness in absorption of system I relative to system II[8] is another clue to the forbidden nature of system I, which will be discussed further in Sec. IV.

C. Rotational analysis

Because the method of combination differences was largely inapplicable directly to the extensively overlapped lines in most of the emission bands of system I, we performed the rotational analyses in the following way:

(a) Provisionally, we assumed the electronic assignment to be ${}^3\Sigma_u^+ - {}^1\Sigma_g^+$, that spin splittings in the upper state were small or negligible, so that the upper state levels could be represented by Eq. (1).

(b) Except for the constant D_0'' (see Sec. III D 1) we adopted the values of B_v'' and D_v'', which had been carefully determined iteratively by Colbourn and Douglas,[5] who then fitted their results to an equation of the same form as Eq. (1).

(c) For each emission band studied, calculated spectra were obtained by applying Eq. (1) to the upper and ground states:

$$\nu(P,R) = \nu_0 + (B_v' + B_v'')m + (B_v' - B_v'' - D_v' + D_v'')m^2 - 2(D_v' + D_v'')m^3 - (D_v' - D_v'')m^4 \qquad (2)$$

with $m=-J$ for a P branch and $m=J+1$ for an R branch.

(d) For an assumed experimental assignment of P and R branches, the constants in Eq. (2) were determined by a quartic least squares fitting program which permitted, by means of a Lagrange multiplier technique, constrained values to be inserted for up to as many as any three of the constants occurring in Eq. (2). Many trial assignments and combinations of constrained constants were tried for a given band. Care was taken to ensure that calculated and observed band head positions matched well. Details of the analyses of the individual bands are presented in Sec. III D.

TABLE I. Molecular constants[a] (cm^{-1}) obtained from rotational analysis of the emission spectrum of Ar_2, $^3\Sigma_u^+ - X\,^1\Sigma_g^+$.

v'	v''	Band origin	B'	$10^6 D'$	$\Delta G(v'+\frac{1}{2})$[b]	$\Delta G(v''+\frac{1}{2})$[c]
$v+1$	1	~93 145.40[d]	~0.055[d]	~1.0[d]		
v	0	93 123.84	0.0732	1.87		25.50
	1	93 096.34			~47.06[d]	20.40
	2	93 077.94				
$v-1$	0	93 056.64	0.0801	0.52	67.20	25.53[e]
	1	93 031.11[e]			67.23	
$v-2$	0	92 974.55	0.0865	0.29	82.09	25.61
	1	92 948.94				20.40[f]
	2	92 928.54[f]				
$v-3$	0	92 878.72	0.0918	0.10	95.83	25.58
	1	92 853.14			95.80	20.32
	2	92 832.82			95.72	15.23[g]
	3	92 817.59[g]				
$v-4$	0	92 771.09	0.0964	1.00	107.63	25.49
	1	92 745.60			107.54	20.41
	2	92 725.19			107.63	15.23
	3	92 709.96			107.63	
$v-5$	0	92 652.77	0.1015	0.83	118.32	25.57
	1	92 627.20			118.40	20.50
	2	92 606.70			118.49	
$v-6$	0	92 524.26	0.1051	0.30	128.51	25.41
	1	92 498.85			128.35	20.37
	2	92 478.48			128.22	

[a]The constants in the table are those used to fit the emission spectrum and some are given to higher accuracy than justified (see Sec. III.C of the text). The ground state constants (cm^{-1}) $B_0'' = 0.05778$, $B_1'' = 0.0534$, $B_2'' = 0.0485$, $B_3'' = 0.0428$, and $D_1'' = 1.66\times10^{-6}$, $D_2'' = 2.0\times10^{-6}$, $D_3'' = 3.3\times10^{-6}$ of Colbourn and Douglas were also used. The value $D_0'' = (0.83\pm0.3)\times10^{-6}$ obtained from the $(v-2, 0)$ emission band was used in preference to the value $D_0'' = 1.13\times10^{-6}$ of Colbourn and Douglas (see Sec. III.D.1 of the text and Fig. 4).

[b]The average values of $\Delta G(v'+\frac{1}{2})$ for $v' = v$ through $v-6$ are 47.1, 67.2, 82.1, 95.8, 107.6, 118.4, and 128.4 cm^{-1}.

[c]See Sec. III.C of the text.

[d]See Sec. III.D.7 of the text.

[e]Our average value of $\Delta G(\frac{1}{2}) = 25.53$ cm^{-1} is used to obtain the origin of this weak band.

[f]Our average value $\Delta G(\frac{3}{2}) = 20.40$ cm^{-1} is used to obtain the origin of this weak band.

[g]Our value $\Delta G(\frac{5}{2}) = 15.23$ cm^{-1} is used to obtain the origin of this weak band.

The results of the rotational analysis are given in Table I and in Fig. 1, where a densitometer trace of the emission spectrum is shown together with line assignments calculated from the constants in Table I. The centrifugal distortion coefficients D' are not accurately determined ($\pm\sim0.5\times10^{-6}$ cm^{-1}), and not much physical significance should be attached to their values, which were found to depend sensitively on the number and accuracy of measurement of the high J lines (which are often weak and overlapped) included for their calculation. Owing to the smallness of the rotational constants of the ground and excited states in relation to the resolution available, there is much overlapping of low J lines and B' values cannot be determined essentially from low J lines alone; unfortunately, errors in D' and B' are correlated, and we estimate that the accuracy of B' ($v' = v$ through $v-6$) is approximately ±0.001 cm^{-1}. A plot of B' vs v' is shown in Fig. 2. The present ground state vibrational spacings $\Delta G(\frac{1}{2}) = 25.5_3\pm0.2$ cm^{-1} and $\Delta G(\frac{1}{2}) = 20.4_0\pm0.2$ cm^{-1} are in good agreement with the values $\Delta G(\frac{1}{2}) = 25.5_6$ cm^{-1} and $\Delta G(\frac{1}{2}) = 20.4_4$ cm^{-1} determined previously from absorption band head measurements,[8] and are also in good agreement with the values $\Delta G(\frac{1}{2}) = 25.7_4\pm0.1$ cm^{-1} and $\Delta G(\frac{1}{2}) = 20.4_1$ cm^{-1} obtained by Colbourn and Douglas.[5] The excited state vibrational spacings $\Delta G(v'+\frac{1}{2})$, $v' = v$ through $v-6$, in Table I are estimated to be accurate to about ±0.2 cm^{-1} and are plotted in Fig. 3.

The observed wave numbers of the emission spectrum in the region 93 150–92 712 cm^{-1} (1073.5–1078.6 Å) are listed in Tables II–IV, together with rotational quantum number assignments based on the constants of Table I, and visual intensity estimates. The goodness of fit of calculated to observed frequencies is indicated in several footnotes to Tables II–IV.

D. Significant features of the emission bands

1. The $(v-2, v'')$ bands

We began the rotational analysis with the band $(v-2, 0)$, which has its bandhead at 1075.56 Å, because this band has the simplest looking rotational structure (Fig.

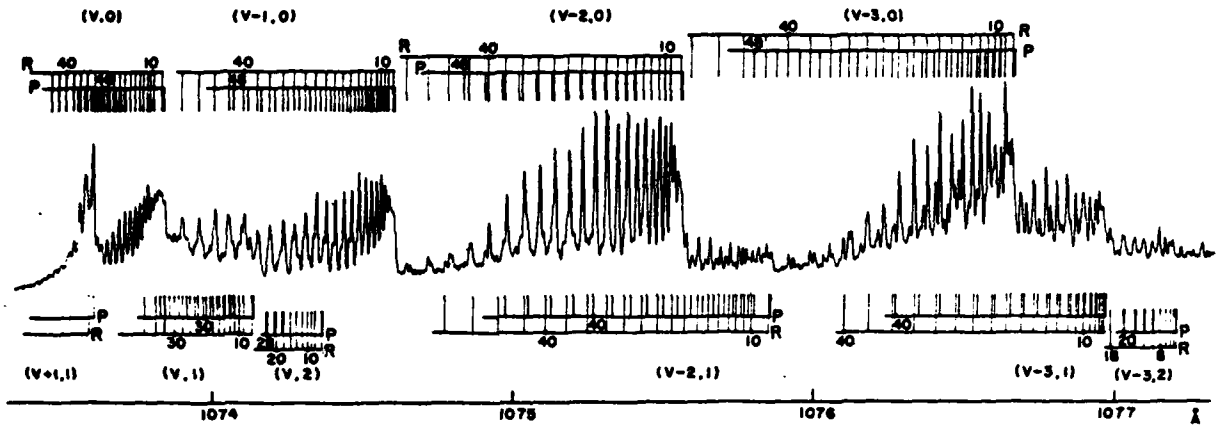

FIG. 1. Densitometer trace of the emission spectrum of system I of Ar_2, $^3\Sigma_u^+ - X\,^1\Sigma_g^+$, from its lowest excited state to the ground state, in the region 1073.5–1077.2 Å. The positions of the straight lines showing the rotational quantum number assignments are calculated from the constants in Table I. In a given band the calculated P branch line of longest wavelength represents the calculated P branch bandhead, and the calculated R branch line of longest wavelength is $R(0)$. For clarity, some low J assignments are omitted from the figure. See Table II for more complete assignments. For the $(v+1, 1)$ band, only the calculated positions of the P branch bandhead and of $R(0)$ are shown (see Sec. III. D7 of the text).

1). On the assumption that only one P branch and one R branch are to be expected (see Sec. III B) and that only even numbered J'' lines are present (since the ^{40}Ar nucleus is a boson with zero nuclear spin), we employed the standard methods of combination differences to test various rotational assignments. The assumption that each single emission peak of the $(v-2, 0)$ band in Fig. 1 corresponds to a single R or P line was tested for various J numberings; the plots of $\Delta_2F/4(J+\frac{1}{2})$ vs $(J+\frac{1}{2})^3$ deviated somewhat more from linearity than expected and yielded approximate B'_{v-2} values in the range 0.17–0.19 cm^{-1}. The assignments leading to these B'_{v-2} values are rejected because there are two agruments for believing these values are too large. The first is that a spectroscopic analysis[12] of the *ab initio* calculated potential curve (configuration interaction approximation) for the upper state of system I[13] yields B'_v values that decrease montonically from $B'_0 = 0.142$ cm^{-1} to $B'_{25} = 0.090$ cm^{-1}, and the second, depending on a comparison with B' values of the upper state of system II, will be given in Sec. IV. On the other hand, if we assume that each individual emission peak in the $(v-2, 0)$ band arises from the almost complete coincidence of a P and R line, then further combination difference tests reveal that for the assumed coincidences $R(J) = P(J+6)$, the values $B'_{v-2} = 0.089$ and $B'_0 = 0.059$ cm^{-1} are obtained (see Fig. 4). This approximate B'_0 value is in substantial

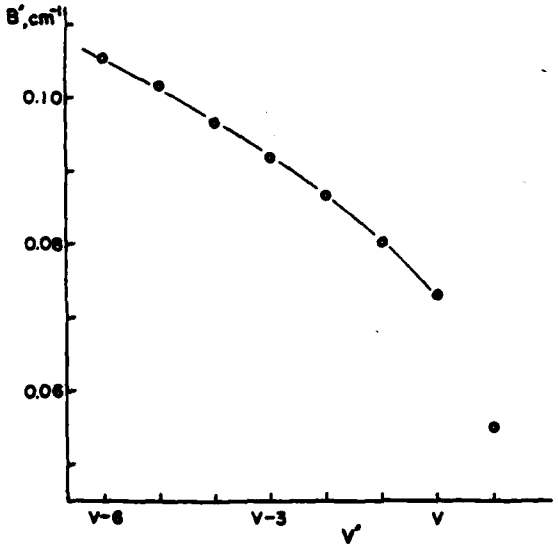

FIG. 2. Plot of B' vs v' for the upper state, $^3\Sigma_u^+$, of system I of Ar_2. For the point B'_{v-1}, see Sec. III. D7 of the text.

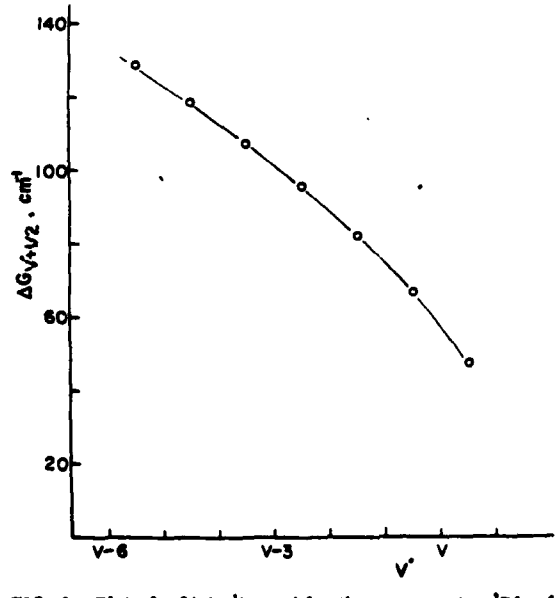

FIG. 3. Plot of $\Delta G(v'+\frac{1}{2})$ vs v' for the upper state, $^3\Sigma_u^+$, of system I of Ar_2.

TABLE II. Observed wave numbers[a] and assignments for the emission spectrum of Ar_2, $^1\Sigma_u^+ - X\,^1\Sigma_g^+$, in the region 1073.53–1074.61 Å.

Observed line (cm^{-1})	I[b]	$(v,0)$[c] J_R	J_P	$(v,1)$[d] J_R	J_P	$(v,2)$[e] J_R	J_P	$(v-1,0)$[f] J_R	J_P
93150.97	2	40							
149.61	3	38							
147.81	5	36	48						
146.16	6		46						
145.94	6								
145.41*B*	5	34							
143.96	7	32	44						
142.75	3		42						
141.54	3	30	40						
139.90	3	28	38						
138.18	3	26	36						
136.52	4	24	34						
134.87	4	22	32						
133.36	5	20	30						
131.87	4	18	28						
130.53	5	16	26						
129.25	5	14	24						
129.09*B*	4			36					
128.18	5	12	22						
127.16	5	10	20						
126.14	5	8	18	34					
125.58	5	6	16						
125.02	5	4	14						
124.42	5	2	12						
124.00	5	0	10						
123.51	5			32					
121.99	2				38				
120.61	2			30					
119.48*B*	2				36				
118.22	3			28				48	
117.00*B*	2				34				
114.82*B*	3				32				
113.45	4			24				46	
112.68*B*	2				30				
110.55*B*	2				28				
109.50*B*	3			20					
108.80	5			18	26			44	
106.77	2			16	24				
105.02	5			14	22			42	
104.50*B*	3			12	20				
103.69*B*	2								48
102.07*B*	3			10	18				
101.11*B*	2			8	16				
100.44	4			6	14			40	
098.85	2			2	10				46
097.36*B*	3						30		
096.55	2							38	
093.40*B*	3					22	28		
092.99	4							36	
090.36*B*	3					20	26		42
089.33*B*	3					18	24		
089.08	4							34	
086.79*B*	3					16	22		40
086.37*B*	3								
085.83	3					14	20	32	
084.80*B*	2								38
083.30*B*	3					12	18		
082.62	4					10	16	30	
081.49*B*	2					8	14		36
080.36	2					6	12		
079.52	5					4	10	28	
077.85*B*	3								34
076.76	5							26	
074.95*B*	3								32

TABLE II (*Continued*)

Observed line (cm^{-1})	I[b]	$(v,0)$[c] J_R	J_P	$(v,1)$[d] J_R	J_P	$(v,2)$[e] J_R	J_P	$(v-1,0)$[f] J_R	J_P
93074.08	4							24	
072.48*B*	2								30
071.64	5							22	
070.12*B*	3								28
069.37	5							20	
068.02*B*	3								26
067.25	5							18	
065.96*B*	3								24
065.33	5							16	
064.16*B*	3								22
063.66	5							14	
062.16	5							12	
060.80	5							10	
059.60	5							8	
058.63	4							6	
057.89	4							4	
057.48	4							2	

[a] All wave number entries are averages obtained from measurements on at least three spectrograms. The letter *B* following a wave number indicates that the line is observed as a shoulder. Individual line assignments were not attempted for the $(v+1,1)$ band (see Sec. III D 7 of the text.

[b] Visual estimates of intensities obtained from a densitometer trace; $I=10$ is arbitrarily assigned to the strongest line observed in the region 1073.5–1078.6 Å.

[c] Calculated P branch bandhead at 93123.56 cm^{-1}. The mean deviation between calculated and observed frequencies with $J \leq 40$ is 0.17 cm^{-1} for the R branch lines and 0.24 cm^{-1} for the P branch lines.

[d] Calculated P branch bandhead at 92098.17 cm^{-1}.

[e] Calculated P branch bandhead at 93077.80 cm^{-1}.

[f] Calculated P branch bandhead at 93056.45 cm^{-1}. The mean deviation between calculated and observed frequencies with $J \leq 40$ is 0.08 cm^{-1} for the R branch lines and 0.46 cm^{-1} for the P branch lines.

agreement with the carefully determined value $B_0'' = 0.05778$ cm^{-1} derived by Colbourn and Douglas[5] by an iterative procedure using, *inter alia*, their absorption spectrum of system II; but their value $D_0'' = 1.13 \times 10^{-6}$ cm^{-1} (corresponding to the broken line in Fig. 4) seems a little too large and we adopted the value $D_0'' = 0.83 \times 10^{-6}$ cm^{-1} (corresponding to the solid line in Fig. 4). Our approximate B_{v-2}' value is of the magnitude expected for a rotational constant of a high lying vibrational level of the upper state of system I. The approximate coincidence $R(J) = P(J+6)$ holds well for calculated lines up to $\sim R(20)$, but experimental resolution of $P(J+6)$ from $R(J)$ occurs first at $J=30$ (see Table II). In agreement with our discussion in Sec. III B, the R branch is assigned as stronger than the P branch, and at higher J values the main peaks are assigned as $R(J)$ and the shoulders on their short wavelength sides as $P(J+6)$. $R(J)$ lines are observed up to $R(48)$. The broadness of the highest few $R(J)$ lines may result from the quasi-bound nature of the ground state levels with high J'' ($40 \leq J'' \leq 48$, according to Colbourn and Douglas[5]). In the absorption spectrum of system I, $R(42)$ is observed to be quite intense but $R(44)$ is very weak, probably as

TABLE III. Observed wave numbers[a] and assignments for the emission spectrum of Ar_2, $^3\Sigma_u^+ - X\,^1\Sigma_g^+$, in the region 1074.61–1076.65 Å.

Observed line (cm^{-1})	I^b	$(v-1,1)^c$		$(v-2,0)^d$		$(v-2,1)^e$		$(v-2,2)^f$		$(v-3,0)^g$		$(v-3,1)^h$	
		J_R	J_P	J_R	J_P	J_R	J_P	J_R	J_P	J_R	J_P	J_R	J_P
93 063.83	1			48									
062.61	1												
047.53	2			46									
046.57	1												
042.83	1												
041.20	2	16	22	44									
040.66B	2												
036.84	1				48								
035.50	3	10	16	42									
035.11	3	8	14										
031.29B	3				46								
030.04	4			40									
026.04B	3				44								
024.96	5			38									
021.07B	3				42								
020.04	6			36									
016.15B	3				40								
015.51	6			34									
014.47B	3					40							
012.71B	3												
012.12B	5				38								
011.74B	5						44						
011.19	7			32									
008.75B	2												
007.76B	4				36								
007.04	7			30		38							
005.93B	3						42						
003.26	8			28	34								
92 999.61	8			26	32		40						
996.34	9			24	30	34							
993.22	7			22	28								
991.23B	3					32							
990.37	8			20	26								
987.70	8			18	24								
986.21B	5					30							
985.37	8			16	22								
983.19	8			14	20								
981.32	9			12	18	28							
979.57	8			10	16		32						
978.02	8			8	14	26							
977.05	7			6	12								
975.84	6			4	10								
975.32	6			2	8		30						
974.90	5			0	6								
973.65	3					24							
971.96	2						28				48		
970.05	3					22							
968.18	2						26						
966.69	3					20							
965.05	2						24						
963.69	2					18					46		
962.27	2						22						
960.94	3					16							
959.78	1						20						
958.47	3					14							
957.24	3						18				44		
956.28	3					12							
954.40	2					10							
952.77	3					8							
951.47	2					6							
950.46	3					4					42		
949.58	2					2							
949.10	3					0							
944.66	2										40		
937.99	3										38		

TABLE III (*Continued*)

Observed line (cm^{-1})	I^b	$(v-1,1)^c$		$(v-2,0)^d$		$(v-2,1)^e$		$(v-2,2)^f$		$(v-3,0)^g$		$(v-3,1)^h$	
		J_R	J_P	J_R	J_P	J_R	J_P	J_R	J_P	J_R	J_P	J_R	J_P
92 936.57	3							12	16				
933.86	2							10	14				
932.16	3								12	36			
931.31*B*	2							6	10				
928.25	3											40	
926.70	4									34			44
925.85	4												
923.11	3										38		
921.21	5									32		38	
918.24	4										36		42
916.61	5									30			
913.98	4										34	36	
912.10	7									28			40
909.22	4										32		
907.79	8									26		34	
905.21	5										30		38
903.90	7									24			
901.63	6										28	32	
900.31	9									22			36
899.21	1												
896.01	4										26		
896.94	8									20			
896.10*B*	5											30	
894.96	6										24		
893.91	8									18			34
892.09	5										22		
891.05	10									16		28	
889.73	5										20		
888.63	9									14			32
887.22*B*	6										18		
886.29	9									12		26	
885.05*B*	6										16		
884.56	7									10			30
882.89	7									8	14		
881.59	10									6	12		
880.58	8									4	10	24	
879.70	8									2	8		28

[a]Same as Footnote a of Table II.
[b]Same as Footnote b of Table II.
[c]Calculated *P* branch bandhead at 93 030.95 cm^{-1}.
[d]Calculated *P* branch bandhead at 92 974.37 cm^{-1}. The mean deviation between calculated and observed frequencies with $J \leq 40$ is 0.06 cm^{-1} for the *R* branch lines and 0.17 cm^{-1} for the *P* branch lines.
[e]Calculated *P* branch bandhead at 92 948.79 cm^{-1}.
[f]Calculated *P* branch bandhead at 93 928.41 cm^{-1}.
[g]Calculated *P* branch bandhead at 92 878.56 cm^{-1}. The mean deviation between calculated and observed frequencies with $J \leq 40$ is 0.10 cm^{-1} for the *R* branch lines and 0.24 cm^{-1} for the *P* branch lines.
[h]Calculated *P* branch bandhead at 92 853.00 cm^{-1}.

a result of predissociation in the ground state. The $(v-2,1)$ band is so weak that its interference in the region of the $(v-2,0)$ band is negligible (Fig. 1). A Fortrat diagram of the $(v-2,0)$ band is shown in Fig. 5.

2. The (v-3, v'') bands

Because of strong hot bands overlapping it, the $(v-3,0)$ appears to be the strongest band observed in emission, and its most striking aspect is the apparently anomalous intensity distribution among the lines giving rise to a band that looks as if it exhibits a kind of "intensity alternation." The main peaks are assigned as $R(J)$ lines of the $(v-3,0)$ band and the considerably weaker lines between $R(J)$ and $R(J+2)$ are assigned as $P(J+6)$. Some of the stronger R lines of $(v-3,0)$ are also enhanced in intensity by contributions from R lines of the relatively strong $(v-3,1)$ band. The above two effects account for the apparently anomalous intensity pattern. For $J>40$ the $R(J)$ lines of $(v-3,0)$ are weak and overlap the weak $(v-2,1)$ band. In the $(v-3,1)$ band the main peaks on the long wavelength side of the $(v-3,0)$ band head are also assigned as $R(J)$ lines and the weaker lines between $R(J)$ and $R(J+2)$ are $P(J+6)$ lines. In the weaker $(v-3,2)$ band the observed intensi-

TABLE IV. Observed wave numbers[a] and assignments for the emission spectrum of Ar_2, $^3\Sigma_u^+ - X\,^1\Sigma_g^+$, in the region 1076.65–1078.62 Å.

Observed line (cm^{-1})	I^b	$(v-3,1)^c$		$(v-3,2)^d$		$(v-3,3)^e$		$(v-4,0)^f$		$(v-4,1)^g$		$(v-4,2)^h$		$(v-4,3)^i$	
		J_R	J_P	J_R	J_P	J_R	J_P	J_R	J_P	J_R	J_P	J_R	J_P	J_R	J_P
92 887.33	6	22													
876.98B	6														
875.67	5		26												
873.72B	6			28?											
873.48	6	20													
871.93	4		24												
870.00	7	18													
868.71	5		22	26	30										
866.87	6	16													
865.82B	5		20												
864.01	7	14		24	28										
863.30B	5		18												
861.57	6	12													
860.23B	5		16												
859.34	6	10		22	26										
857.54	5	8													
855.90	6	6													
854.77	6	4		20	24										
853.97	5	2													
851.77	4			18											
851.06B	3				22										
848.12	4			16											
847.60	4				20										
844.71	4			14	18										
842.11	4			12	16										
839.54	3			10	14										
837.66	4			8	12										
835.84	4			6	10										
834.52	3			4	8										
833.66	2			2	6										
831.21	2					14	18								
825.20	3					*10*	*14*			40	44				
820.89	3					6	10		38?						
819.29	3					4	8								
818.01	4					2	6	32		38					
815.86	3								36?						
813.83	4											40			
813.04	4							30							
810.63	4								34	36	40				
808.71	4														
807.77	4							28							
806.03	4								32			38			
803.81	5							26		34	38				
801.29									30						
799.47	6							24					40		
797.15	5								28	32	36	36			
795.31	6							22							
793.27	6								26						
791.51	7							20		30	34		38		
789.60	5								24			34			
787.89	7							18							
786.20	7								22	28	32				
785.04	8							16							
783.40	6								20			32	36	34	
782.15	9							14							
780.81B	7								18	26	30				
779.76	8							12							
778.80	7								16						36
777.37	8							10					34		
775.86	8							8		24	28	30		32	
774.19	7							6							
772.34	10							4	8						
771.87B	8							2	6	22	26				
768.14	8									20					
767.48	7										24			30	

TABLE IV (*Continued*)

Observed line (cm^{-1})	J^a	$(v-3,1)^c$ J_R	J_P	$(v-3,2)^d$ J_R	J_P	$(v-3,3)^e$ J_R	J_P	$(v-4,0)^f$ J_R	J_P	$(v-4,1)^g$ J_R	J_P	$(v-4,2)^h$ J_R	J_P	$(v-4,3)^i$ J_R	J_P
92 766.28	7														
764.26	9											26	30		
763.85*B*	7									18					
763.42*B*	8										22				
762.91*B*	7														32
760.73	10									16					
760.48	10										20			28	
757.68	9									14					
754.96	10									12					
754.06*B*	8										16	22	26	26	
752.46	9									10	14				
750.41	10									8					
749.30	9											20	24		28
748.98	9									6	10				
747.30	9									4	8			24	
746.13	9									2	6				
745.30	8									0	2	18	22		
743.46	7														26
742.08	8													22	
741.39	8											16	20		
738.49	8														24
738.08	9											14	18		
735.54*B*	7														
735.30	8											12	16		
735.10*B*	7														
733.10*B*	7														22
732.75	8											10	14	18	
730.40	7											8	12		
728.53	8											6	10	16	20
727.17	7											4	8		
725.88	7											2	6		
724.92	7											0	2		18
723.46	6														
721.10	6													12	16
718.05	6													10	14
715.54	6													8	12
713.40	6													6	10
711.88	6													4	8

[a]Same as Footnote a of Table II.
[b]Same as Footnote b of Table II.
[c]Calculated *P* branch bandhead at 92 853.00 cm^{-1}.
[d]Calculated *P* branch bandhead at 92 832.71 cm^{-1}.
[e]Calculated *P* branch bandhead at 92 817.45 cm^{-1}.
[f]Calculated *P* branch bandhead at 92 770.94 cm^{-1}.
[g]Calculated *P* branch bandhead at 92 745.47 cm^{-1}.
[h]Calculated *P* branch bandhead at 92 725.09 cm^{-1}.
[i]Calculated *P* branch bandhead at 92 709.90 cm^{-1}.

ty pattern is explained by the near coincidence of $R(J)$ and $P(J+4)$ lines.

3. *The (v-4, v'') bands*

For $v'=v$, $v-1$, $v-2$, $v-3$, the $(v',0)$ bands are stronger than their associated hot bands, but for $v'=4$ the $(v-4,1)$ is stronger than $(v-4,0)$. In addition there is present, towards the long wavelength end of the v'' progression, a dissociation continuum, which can be seen in Fig. 5 of Ref. 7. There is considerable overlapping among the lines of the $(v-4,v'')$ bands. The overall intensity pattern observed, especially the occurrence of strong peaks, is explicable in terms of assignments in the individual bands in which the R branches are stronger than the P branches.

4. *The (v-5, v'') and (v-6, v'') bands*

In emission the increased intensity of the dissociation continuum relative to the discrete emission and serious overlapping problems render the analysis more difficult. We have examined the above bands in absorption, where the continuum is absent, but overlapping makes the visual identification of band heads and their matching with calculated heads difficult. The spectroscopic constants in Table I for these bands may be less reliable than for the other bands studied.

5. *The (v-1, v'') bands*

Since the $(v-1,1)$ band is too weak to be studied, the $(v-1,0)$ band is free from overlapping by other bands

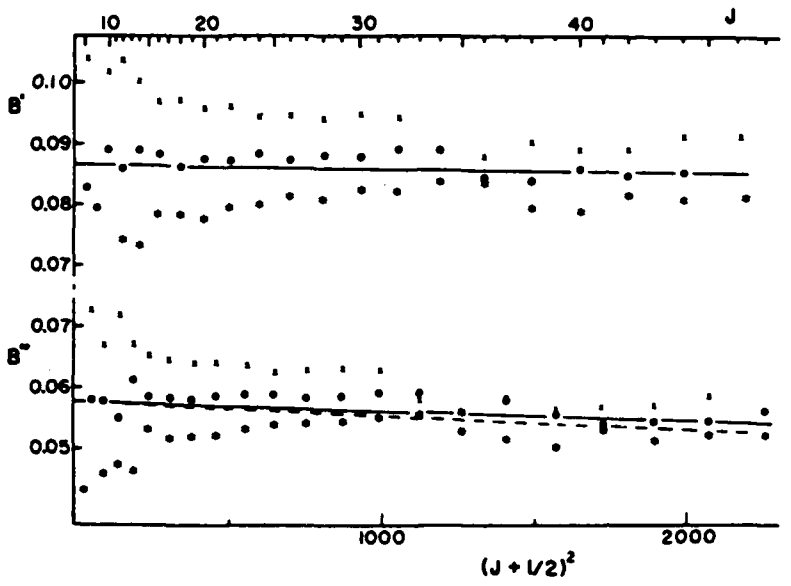

FIG. 4. Plots of $\Delta_2F/4(J+\frac{1}{2}) = B$ vs $(J+\frac{1}{2})^2$ for the upper and ground states of the $(v-2, 0)$ band of system I of Ar_2. Circles refer to the final J assignment chosen and shown in Fig. 1 and Table III; crosses and asterisks refer, respectively, to a decrease and increase by 2 in that J assignment. For the ground state the solid line corresponds to the B_0'' and D_0'' values in Table I, and the broken line corresponds to the B_0'' and D_0'' values of Coulbourn and Douglas[5] (see Sec. III. D. 1 of the text). For the upper state the solid line corresponds to the $B'_{v'-2}$ and $D'_{v'-2}$ values in Table I. The sudden decrease in B' or B'' occurs at the point at which the P line is first resolved experimentally from the nearby stronger R line (see Table III).

between its band head and that of the $(v, 2)$ band. Between these two bands heads the R branch is stronger than the P branch, and the main peaks are assigned as $R(J)$ and the shoulders on their short wavelength sides as $P(J+8)$. In the region of the hot bands $(v, 2)$ and $(v, 1)$ the line structures become broader and more complicated, but the main peaks are assigned as $R(J)$ of $(v-1, 0)$ up to $J=48$, which is, according to Colbourn and Douglas,[5] the highest quasibound level in the $v''=0$ ground state. If the line $R(50)$ existed, its calculated position shows that it would be obscured by the bandhead of the $(v, 0)$ band.

6. The (v,v'') bands

The line structures of the $(v, 0)$ band are tightly spaced and, except near the bandhead, look fairly symmetrical. The observed lines were assigned on the assumption that $R(J) = P(J+10)$ for $J=0-30$, and the calculated lines $R(J)$ and $P(J+10)$ differ at most by 0.6 cm^{-1}. Beyond $J=30$ the lines merge with those of the $(v+1, 1)$ band. The hot bands $(v, 1)$ and $(v, 2)$ are weak but their presence can be seen in Fig. 1, together with the calculated line positions.

7. The (v+1, v'') bands

The bandhead of the $(v+1, 0)$ band was observed weakly in emission at 93 177.5 cm^{-1} (1073.22 Å) with a 2 m spectrograph[7] but this band is too weak to be analyzed at high resolution.

The stronger $(v+1, 1)$ band is observed at high resolution in both emission and absorption, but only seven rotational structures which span the range 93 143.96–93 150.97 cm^{-1} are seen in emission.[14] The feature of longest wavelength at 93 143.96 cm^{-1} is very close in energy to the interval 93 143.80 cm^{-1} corresponding to

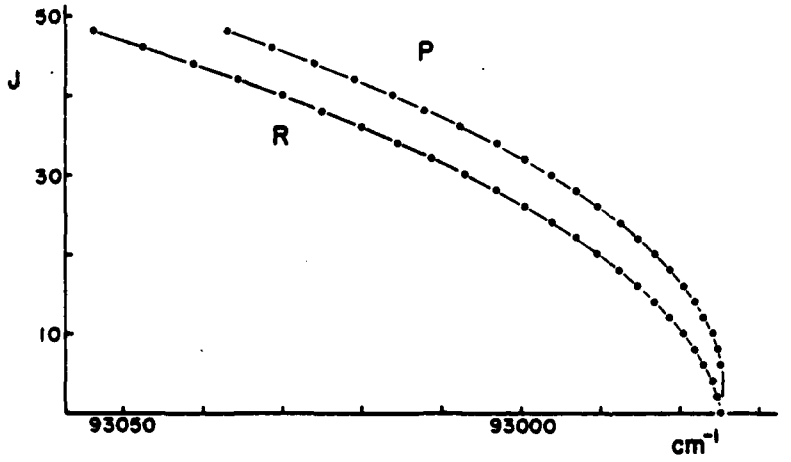

FIG. 5. A Fortrat diagram for the $(v-2, 0)$ band. The dots represent observed frequencies (Table III), and the curves are calculated from Eq. (2) with the constants from Table I. Note that frequency is plotted against J, not $|m|$. Experimental resolution of $R(J)$ from $P(J+6)$ first occurs at $J=30$ (see also Table III and Fig. 4).

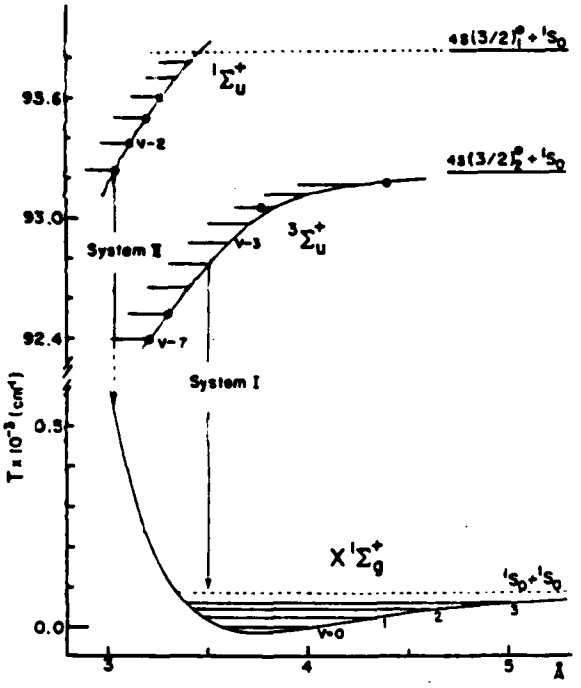

FIG. 6. Potential energy curves for the first ($^3\Sigma_u^+$) and second ($^1\Sigma_u^+$) excited states of Ar_2 and for the ground state ($X\,^1\Sigma_g^+$). The ground state curve and its energy levels are accurately known. The excited state curves are schematic but the energy levels shown are accurately known; the estimation of the outer turning points, represented by circles, of some of these levels and the positions of the excited state curves relative to each other and to the ground state curve are discussed in Sec. IV of the text. Note that one scale division represents 100 cm^{-1} for the ground state and 200 cm^{-1} for the excited states.

the forbidden transition Ar^*, $4s(3/2)_1^0$–Ar, $3p^6\,^1S_0$, but the observed feature (Fig. 1) does not have the appearance expected of a forbidden atomic line; the forbidden line, if present, is too weak to be identified in the present experiment. A detailed rotational analysis of the seven structures observed is not feasible, especially since high J lines of the $(v, 0)$ band are also in this region. The upper state of the $(v+1, 1)$ band lies less than 60 cm^{-1} below the dissociation limit $4s(3/2)_1^0 + 3p^6\,^1S_0$, so that predissociation of the upper state of this band is a possibility which may account for our observation of rotational structures extending only 7.0 cm^{-1} to the high energy side of the bandhead. According to our discussion (Sec. IV) of the intensity of the $(v+1, 1)$ band, the outer turning point of the $v' = v+1$ level is expected at considerably greater internuclear distance than that of the $v' = v$ level, so that B'_{v+1} may be less than the value 0.066 cm^{-1} which would correspond to extrapolation of the curve in Fig. 2. If we assume $B'_{v+1} = 0.055$ cm^{-1} then levels with $J' \leq 31$ lie below the dissociation limit, and Eq. (2) with $\nu_0 = 93\,145.4$ cm^{-1}, $D'_{v+1} = 1 \times 10^{-6}$ cm^{-1}, $B''_1 = 0.0534$ cm^{-1}, and $D''_1 = 1.66 \times 10^{-6}$ cm^{-1} yields $R(30) = 93\,150.8$ cm^{-1} located 6.8 cm^{-1} to the high energy side of the bandhead. Thus, a low value of B'_{v+1} (~0.055 cm^{-1}) and the predissociation of lines with $J' > 31$ provides a tentative interpretation of the observations. A detailed explanation of the intensity pattern of the many overlapping lines in the 7.0 cm^{-1} interval has not been attempted, and we note that the above interpretation depends on the somewhat questionable assumption of the validity of Eq. (2) close to the dissociation limit.

IV. DISCUSSION

We have attempted in Fig. 6 to use the spectroscopic results of the present work and of Ref. 7 to portray the general shapes and positions of the first two excited states of Ar_2 relative to each other and relative to the ground state. The ground state curve is accurately known in the region of its bound vibrational levels and was constructed from the data in Table II of Colbourn and Douglas[5]; the repulsive branch above the dissociation limit was obtained from the Morse–Spline–van der Waals potential (MSV-III) of Parson, Siska, and Lee.[15] The portions of the potential curves shown for the $^3\Sigma_u^+$ and $^1\Sigma_u^+$ states are schematic. The energy positions shown for their bound vibrational levels are accurately determined, and the methods of estimating the outer turning points of some of these levels will emerge in those parts of the following discussion concerned with observed intensities and the discrete or diffuse nature of various bands.

The similarity in the absorption and emission intensities of the band heads belonging to a given v'' progression has been noted previously.[7] The general pattern of the intensities of the bands given in Table II of Ref. 7 deserves further attention. First, however, we note that the estimated intensities in Table II of Ref. 7 refer to bandheads. In the rotationally resolved spectra we obtained at higher resolution it is very difficult to estimate even semiquantitatively, because of overlapping and other effects, the integrated band intensities of weak hot bands $(v', v'' \neq 0)$ relative to $(v', 0)$, but we believe the bandhead values of weak hot bands overestimate these relative intensities, sometimes considerably; it is also difficult in some cases to estimate intensities of the $(v', 0)$ bands (see, for example, Sec. III D 2).

For $v' = v+1$ the hot band $(v', 1)$ is markedly more intense than the band $(v', 0)$, whereas for $v' = v$, $v-1$, $v-2$, or $v-3$ the reverse is observed (see Fig. 1). This suggests that the $(v+1, 1)$ band originating from the highest observed level of the upper state terminates on the ground state near the outer classical turning point of the $v'' = 1$ level which is at $R'' = 4.39$ Å (see Fig. 6); the $(v+1, 0)$ band is therefore expected to be much weaker since $R''_e = 3.75$ Å. If a $(v+1, 2)$ transition occurred near the outer turning point of the $v'' = 2$ level, the band would be expected to be weaker than the $(v+1, 1)$ band, and its position is such that it would be obscured in the intense bandhead region of the strong $(v, 0)$ band. For $v' = v$ the bands $(v, 1)$ and $(v, 2)$ may perhaps correspond to transitions occurring near the outer turning points $v'' = 1$ and 2, respectively, in the ground state; but the much higher intensity of the $(v, 0)$ band (Fig. 1) indicates that R'_v is considerably smaller than R'_{v+1} (Fig. 6). For $v' = v-1$ the extreme weakness in emission of $(v-1, 1)$ relative to $(v-1, 0)$ suggests that the $(v-1, 0)$ transition occurs at $R \simeq R''_e$. For $v' < v-1$ it seems likely that the

hot bands observed correspond to transitions with $R < R_e''$ which terminate near the inner classical turning points on the ground state potential curve. This is consistent with the observation that as v' decreases from $v' = v - 1$ the number of hot bands generally increases,[16] and that for $v' \leq v - 4$ the $(v', 1)$ band is stronger than the $(v', 0)$ band. At $v' = v - 4$, bands with $v'' = 0$–4 are observed in emission, and towards the long wavelength end of this v'' progression, a dissociation continuum first becomes apparent.

From the ground state potential[5] we estimate that the dissociation asymptote crosses the inner wall at $R = 3.35_3$ Å and that at $v'' = 4$ the location of the inner turning point is only ~0.02 Å greater. As v' decreases from $v - 4$ to $v - 7$ the diffuse structureless bands of the dissociation continuum increase in intensity relative to the discrete emission bands, as would be expected. If we assume that the diffuse emission band from the level $v - 6$ or $v - 7$ is a vertical transition terminating on the repulsive branch of the ground state curve, the energy difference between the estimated peak of that diffuse emission band and the discrete emission or absorption band $(v - 6, v'')$ or $(v - 7, v'')$ can be used to calculate how far above the $^1S_0 + {}^1S_0$ asymptote, and consequently at what internuclear distance, the vertical transition occurs. The approximate outer turning points of the $v - 6$ and $v - 7$ levels were obtained in this way (Fig. 6).

Similarly, a possible explanation for the observation that system II exhibits discrete absorption bands but only diffuse emission bands[7] is that the latter correspond to vertical transitions from the bound upper state levels of system II to the repulsive branch of the ground state curve above its dissociation limit, i.e., at $R < \sim 3.35$ Å, whereas the discrete absorption bands $(v', 0)$ correspond to "nonvertical" transitions, since $R_e'' = 3.75$ Å. On this basis, the outer turning points of all the levels $(v - 3)$ through $(v + 2)$ are calculated to lie in the approximate range 3.04–3.35 Å (see Fig. 6). In contrast, the five upper state levels of system I $(v + 1, v, \ldots, v - 3)$ from which only discrete emission bands are observed are therefore expected to have outer turning points at internuclear distances rather greater than 3.35 Å (Fig. 6). This implication, plus the general similarity in the overall shapes of the first and second excited state potentials of Ar_2, and the fact that $B' = 0.1057$ cm^{-1} for the $(v - 3)$ level of the second excited state,[5] suggest that the value $B' = 0.0865$ cm^{-1} (Table I) is more appropriate for the $(v - 2)$ level of the first excited state than a higher value $B' \simeq 0.17$–0.19 cm^{-1} which corresponds to an alternative rotational quantum number assignment (rejected in Sec. III D 1) for the $(v - 2, 0)$ band of system I.

The *ab initio* calculated potential (configuration interaction approximation) for the $^3\Sigma_u^+$ state of Ar_2 of Saxon and Liu[13] was not designed for high accuracy in the long range region corresponding to our observed discrete emission bands, and the calculated rotational constants and vibrational spacings are not thought accurate enough[12] to establish the absolute vibrational numbering in the upper state of system I. The general consistency of the B'_{v-2} value in Table I and those obtained for high lying levels of the calculated $^3\Sigma_u^+$ potential curve has already been cited (Sec. III D 1) in support of our preferred rotational assignment for the $(v - 2, 0)$ band.

The configuration interaction calculation of Saxon and Liu[13] gives the total well depth of the $^3\Sigma_u^+$ state as 5461 ± 1613 cm^{-1} at an internuclear separation $R_e = 2.43$ ± 0.05 Å. This calculation also shows near $R = 4.23$ Å a potential maximum of ~75 cm^{-1} above the dissociation limit. There is no experimental evidence in the absorption spectrum[8] for such a hump. The observed emission bands with discrete structure originate from bound levels $v + 1, \ldots, v - 7$ that lie within the uppermost 1%–15% of that well depth. Gillen *et al.*[17] have interpreted measurements of the scattering of Ar^*, $4s(3/2)_1^0$ by Ar, $3p^6\,{}^1S_0$ in terms of a Morse potential ($D_e = 6291$ ± 323 cm^{-1}, $R_e = 2.33 \pm 0.02$ Å), but as those authors note, no information on the true form of the $^3\Sigma_u^+$ potential far from $R = R_e$ is thereby implied. In fact, our plot of $\Delta G(v' + \frac{1}{2})$ versus v' (Fig. 3) shows slight negative curvature instead of the strict linearity required by a Morse potential. The potential energy curves for the Ar_2 excimer states calculated very recently by Spigelmann and Malrieu[18] show no humps at long range in either of the lowest two curves ($^3\Sigma_u^+$ and $^1\Sigma_u^+$). In their Fig. 1, the shape of the second lowest curve ($^1\Sigma_u^+$) is determined by relatively few calculated points, but that shape does suggest that their $^1\Sigma_u^+$ state would possess bound vibrational levels with outer turning points at $R > \sim 3.35$ Å, whereas the conclusions we draw from the behavior of system II in absorption and emission (and show schematically in our Fig. 6) indicate the opposite. The relationship between the steep slope of the outer branch of the $^1\Sigma_u^+$ curve in our Fig. 6 and the position of the $4s(3/2)_1^0 + 3p^6\,{}^1S_0$ asymptote suggests that a potential hump may exist in the $^1\Sigma_u^+$ state, and this possibility is supported by the previous observation[8] that the five absorption bands of shortest wavelength in system II are somewhat diffuse and terminate above the dissociation limit $4s(3/2)_1^0 + 3p^6\,{}^1S_0$.

If we assume the highest observed level $(v' = v + 1)$ terminating on the outer branch of the $^3\Sigma_u^+$ curve is in the asymptotic region where its binding energy (57.6 cm^{-1}) is given by C_6R^{-6} and use an estimate for C_6 obtained from the experimental atomic polarizabilities[19] and the Slater–Kirkwood formula,[20] then application of the theory for the distribution of vibrational levels near the dissociation limit[21] indicates that nine additional bound vibrational levels should exist between $v' = v + 1$ and the dissociation limit. We have no experimental evidence to support such a conclusion. Moreover, near the highest observed level, the experimental $\Delta G(v' + \frac{1}{2})$ versus v' curve (Fig. 3) shows no positive curvature, and positive curvature is a necessary but not sufficient condition for the applicability of the long-range theory for a C_6R^{-6} potential. In addition, the validity of the Slater–Kirkwood formula (originally derived for closed shell systems) is dubious for the estimation of the C_6 coefficient for the interaction Ar, $3p^6\,{}^1S_0 + Ar^*$, $4s(3/2)_1^0$. With these reservations we conclude tentatively that the outer branch of the $^3\Sigma_u^+$ curve for Ar_2 near the highest observed emitting level is not in the asymptotic C_6R^{-6} region.

As discussed in Sec. III D, the rotational assignments

in the system I bands analyzed show that the intensity patterns observed are accounted for in terms of R branches that are stronger than P branches and the absence of Q branches of observable intensity. This is consistent with an upper state coupling scheme which is intermediate between Hund–Mulliken cases b and c, but which is closer to case b, $^3\Sigma_u^+$ with unresolved spin splittings. Band system II is definitely produced by an allowed transition, $0_u^+(^1\Sigma_u^+) - X\,0_g^+(^1\Sigma_g^+)$, and is stronger in absorption than system I,[8] which, regarded as $^3\Sigma_u^+ - X\,^1\Sigma_g^+$, is spin forbidden. However, according to our previous discussion, the discrete bands of system I will, in general, have more favorable Franck–Condon factors than the discrete bands of system II having the same v'' value (see Fig. 6). This viewpoint is compatible with the observation that system I exhibits the same discrete bands in both absorption and emission and, in addition, shows an oscillatory dissociation continuum in emission only for $v' \leq v - 4$; whereas, in contrast, no discrete bands of system II are observed in emission.[7] The observation[22] that Ne_2 shows no molecular absorption to an upper state derived from $3s(3/2)_2^+ + 2p^6\,^1S_0$ argues against an approximately case c coupling in the Ne_2 upper state of which the 1_u component would give rise to an allowed transition from the $0_g^+(^1\Sigma_g^+)$ ground state; on the other hand, the intercombination system $^3\Sigma_u^+ - {}^1\Sigma_g^+$ is expected to be more strongly forbidden in Ne_2 than Ar_2.

Finally, we consider the effects on the Tesla excited emission spectrum of Ar_2 caused by the addition of excess helium. The principal effect observed is the strong quenching of system II. We speculate that one major process for the formation of an excited electronic molecule, Ar_2^* in the discharge involves three body collisions[23] of the type $Ar^* + Ar + M - Ar_2^* + M$. In pure argon, M = Ar. In a mixture of argon and excess helium the above process with M = Ar or He occurs yielding Ar_2^*, though the predominating three body collisions involving Ar^*, viz., $Ar^* + 2He$, cannot yield Ar_2^* but may permit time for the short-lived[24] Ar^*, $4s(3/2)_1^0$ but not the long lived[25,26] Ar^*, $4s(3/2)_2^0$ to radiate before Ar_2^* is formed by the process Ar^*, $4s(3/2)_2^0 + Ar$, $3p^6\,^1S_0 + M - Ar_2^*(^3\Sigma_u^+) + M$. This preferential radiative destruction of Ar^*, $4s(3/2)_1^0$ is further enhanced in the presence of excess helium because resonance-radiation trapping, which is known to increase its apparent lifetime,[24] is reduced or eliminated. In addition, the quenching of various rare gas atoms from the first resonance level to the lowest metastable level by collision with ground state rare gas atoms has been observed,[3,27] and although the specific process Ar^*, $4s(3/2)_1^0 + He - Ar^*$, $4s(3/2)_2^0 + He$ has not been measured, it may conceivably contribute to the destruction of Ar^*, $4s(3/2)_1^0$. Thus, in a mixture of argon and excess helium the formation of Ar_2^*, $0_u^+(^1\Sigma_u^+)$ is inhibited and system II is quenched. In a mixture of argon with excess neon a somewhat less pronounced quenching of system II of Ar_2 has been observed.[7]

V. CONCLUDING REMARK

A rotational analysis of the emission spectrum of system I of Ar_2 from its lowest excited state to the ground state has led to the assignment of the excited state as approximately $^3\Sigma_u^+$ with triplet splittings too small to be resolved. This assignment in which the coupling scheme is closer to Hund–Mulliken case b than to case c provides a consistent interpretation of the main features of the spectrum. The inclusion in our analysis of system I of the ground state rotational constants obtained by Colbourn and Douglas[5] from the absorption spectrum of system II of Ar_2 corroborates the essential correctness of those ground state rotational constants.

ACKNOWLEDGMENTS

We are grateful to Dr. R. P. Saxon for an unpublished spectroscopic analysis of a calculation reported in Ref. 13, to Dr. A. Dalgarno for the suggestion in Ref. 20, and to Dr. A. E. Douglas for a valuable discussion. We thank Dr. K. Kirby, Dr. J. Burrows, and Dr. W. H. Parkinson for critical readings of the paper. This work was supported by the Air Force Geophysics Laboratory, and by the Air Force Office of Scientific Research (AFSC) under contract F49620-77-C-0010.

[1] C. W. Werner, E. V. George, P. W. Hoff, and C. K. Rhodes, IEEE J. Quantum Electron. QE-13, 769 (1977).
[2] D. C. Lorents, Physica (Utrecht) 82C, 19 (1976).
[3] R. E. Gleason, T. D. Bonfield, J. W. Keto, and G. K. Walters, J. Chem. Phys. 66, 1589 (1977).
[4] R. A. Gutcheck, R. M. Hill, D. C. Lorents, D. L. Huestis, M. V. McCusker, and H. H. Nakano, J. Appl. Phys. 46, 3106 (1975). See also D. H. Stedman and D. W. Setser, J. Chem. Phys. 52, 3957 (1970), and D. H. Stedman and D. W. Setser, Progr. React. Kinet. 6, 194 (1971).
[5] E. A. Colbourn and A. E. Douglas, J. Chem. Phys. 65, 1741 (1976).
[6] D. E. Freeman, K. Yoshino, and Y. Tanaka, J. Chem. Phys. 67, 3462 (1977).
[7] Y. Tanaka, W. C. Walker, and K. Yoshino, J. Chem. Phys. 70, 380 (1979).
[8] Y. Tanaka and K. Yoshino, J. Chem. Phys. 53, 2012 (1970).
[9] G. Herzberg, *Molecular Spectra and Molecular Structure I. Spectra of Diatomic Molecules* (Van Nostrand, New York, 1950), pp. 236, 276.
[10] R. E. Miller, J. Chem. Phys. 43, 1695 (1965).
[11] J. K. G. Watson, Can. J. Phys. 46, 1637 (1968).
[12] R. P. Saxon (personal communication, 1978).
[13] R. P. Saxon and B. Liu, J. Chem. Phys. 64, 3291 (1976).
[14] In Figs. 4 and 5 of Ref. 7 the narrow emission band near 1073.6 Å is the $(v = 1, 1)$ band.
[15] J. M. Parson, P. E. Siska, and Y. T. Lee, J. Chem. Phys. 56, 1511 (1972).
[16] We note that the band $(v - 1, 1)$ is, relative to $(v - 1, 0)$, stronger in absorption than emission; this is contrary to expectation since the Boltzmann population (relevant only in absorption) of $v'' = 1$ is, at 77 °K, only ~0.62 of that of $v'' = 0$. Some of the strong absorption lines in this region may belong to system II rather than to the $(v - 1, 1)$ band of system I.
[17] K. T. Gillen, R. P. Saxon, D. C. Lorents, G. E. Ice, and R. E. Olson, J. Chem. Phys. 64, 1925 (1976).
[18] F. Spiegelmann and J.-P. Malrieu, Chem. Phys. Lett. 57, 214 (1978).
[19] T. M. Miller and B. Bederson, Adv. At. Mol. Phys. 13, 1 (1977).
[20] The Slater–Kirkwood values of the C_6 coefficients for the interactions Ar^*, $4s(3/2)_1^0 + Ar$, $3p^6\,^1S_0$ and Ar, $3p^6\,^1S_0 + Ar$, $3p^6\,^1S_0$ are 1.346×10^6 cm^{-1} Å^6 and 3.266×10^5 cm^{-1} Å^6, respec-

tively. The latter is close to the value 3.132×10^{6} cm^{-1} Å^{6} recommended by A. Dalgarno, Adv. Chem. Phys. 12, 143 (1967). Our estimate of C_6 for the excited state, $C_6 = 1.291 \times 10^{6}$ cm^{-1} Å^{6}, is obtained by multiplying the recommended ground state value by the ratio of the above Slater–Kirkwood values. We thank Dr. Dalgarno for suggesting this method of estimating the excited state C_6 value.

[21]R. J. LeRoy and R. B. Bernstein, J. Chem. Phys. 52, 3869 (1970).

[22]Y. Tanaka and K. Yoshino, J. Chem. Phys. 57, 2964 (1972).

[23]Our intention is to convey not the necessity for truly ternary collisions, but rather that the argon excimer formed initially in a binary collision is subsequently stabilized, by collision with a third body M, against dissociation.

[24]E. Ellis and N. D. Twiddy, J. Phys. B 2, 1366 (1969).

[25]R. S. Van Dyck, Jr., C. E. Johnson, and H. A. Shugart, Phys. Rev. A 5, 991 (1972).

[26]N. E. Small-Warren and L.-Y. C. Chin, Phys. Rev. A 6, 1777 (1975).

[27]R. Atzmon, O. Chesnovsky, B. Raz, and J. Jortner, Chem. Phys. Lett. 29, 310 (1974).